



# Phosphorus attenuation in streams by water-column geochemistry and benthic sediment reactive iron

Zachary P. Simpson<sup>1</sup>, Richard W. McDowell<sup>1,2</sup>, Leo M. Condron<sup>1</sup>

<sup>1</sup>Department of Soil and Physical Sciences, Lincoln University, Lincoln, 7647, New Zealand

5 <sup>2</sup>AgResearch, Lincoln Science Centre, Lincoln, 7647, New Zealand

*Correspondence to:* Zachary P. Simpson (zpsimpso@gmail.com)

**Abstract.** Streams can attenuate inputs of phosphorus (P) and, therefore the likelihood of ecosystem eutrophication. This attenuation is, however, poorly understood, particularly in reference to the geochemical mechanisms involved. In our study, we measured P attenuation mechanisms in the form of (1) mineral (co-)precipitation from the water-column and (2) P sorption with benthic sediments. We hypothesized that both mechanisms would vary with catchment geology and, further, that P sorption would depend on reactive Fe content in sediments. We sampled 31 streams at baseflow conditions, covering a gradient of P inputs (via land use), hydrological characteristics, and catchment geologies. Geochemical equilibria in the water-column were measured and benthic sediments (<2 mm) were analyzed for sorption properties and P and iron (Fe) fractions. Neither P-containing minerals (e.g., hydroxylapatite) nor calcite-phosphate co-precipitation had the potential to occur. In contrast, in-stream dissolved reactive P (DRP) correlated with labile sediment P (water-soluble and easily reduced Fe-P), but only for streams where hyporheic exchange between the water-column and the coarse sediment porewaters was likely sufficient. The non-labile P fractions contained most of sediment P (generally >90%) and varied with parent geology. Similarly, most sediment Fe was in a recalcitrant form (generally >90-95%). However, despite its small contribution to total sediment Fe, the pool of surface-reactive Fe was a strong predictor for sediment P sorption potential. Our results suggest that, in these streams, it is the combination of biogeochemical Fe and P cycles and the exchange with the hyporheic zone that attenuates DRP in baseflow. Such combinations are likely to vary spatiotemporally within a catchment and must be considered alongside inputs of P and sediment if the P concentrations at baseflow – and eutrophication risk – are to be well managed.

## 1 Introduction

The mitigation of phosphorus (P) pollution is necessary to manage the eutrophication of water bodies. The efficacy of mitigation measures is typically hoped for in stream monitoring data – a change within the catchment could decrease export of P downstream – but such effects are easily masked (Meals et al., 2010) due to the many biogeochemical processes integrated into the P signal (Dupas et al., 2018a; Halliday et al., 2012). Once mobilized from land via surface runoff or sub-surface flows (McDowell et al., 2004, 2015), P is repeatedly impeded along its flowpath by biotic and abiotic processes (Huang et al., 2018). This persistence of P gives rise to ‘legacy P’ (Powers et al., 2016; Sharpley et al., 2013), where past P inputs can take unknown



30 years (decades, centuries) to deplete. For example, McCrackin et al. (2018) estimated that only 6% of all anthropogenic P inputs to the Baltic Sea drainage basin for 1900-2013 have discharged into the sea. Knowing the mechanisms behind legacy P will improve predictions of P transport and thus not only engender wise P management but appropriate assessment of management as well.

Legacy P refers to the attenuation – and slow trickle downstream – of P across the entire catchment, but perhaps the most reactive flowpath for P is the stream itself (Ensign and Doyle, 2006; Haggard and Sharpley, 2007). At baseflow, P in streams is subject to biotic and abiotic processes which could lead to the transient storage of P (within the channel or in biota) or its re-mobilization back to the water column (Hall et al., 2013; House, 2003). Both periphyton (Biggs, 2000; Davies and Bothwell, 2012; Hill et al., 2009) and heterotrophic microbes (McDowell, 2003; Mulholland et al., 1997; Muscarella et al., 2014) can assimilate P, especially dissolved reactive P (DRP; mostly orthophosphate but can include labile organic compounds), as it is the most bioavailable P form (Biggs, 2000; Muscarella et al., 2014). The turnover of this assimilated P back to the water column completes one cycle of the biotic P attenuation (or spiraling) mechanism (Ensign and Doyle, 2006; Newbold et al., 1983). Numerous studies on strictly biotic P attenuation, however, conclude that biotic mechanisms are not critical for P attenuation in streams (Griffiths and Johnson, 2018; Hall et al., 2002; Weigelhofer et al., 2018). Instead, abiotic P mechanisms – as influenced by stream biogeochemistry – may be responsible for attenuating P (Jarvie et al., 2006; McDaniel et al., 2009; Stutter et al., 2010). Yet, abiotic (i.e., geochemical) P attenuation phenomena are poorly studied relative to biotic P attenuation. To address this gap, we consider two geochemical mechanisms – calcium (Ca) based (co-)precipitation and sediment P sorption – as the primary components of abiotic P attenuation in streams.

Calcium-phosphate mineral precipitation and  $\text{CaCO}_3$  co-precipitation may remove DRP from the water column given sufficient Ca, pH, and  $p\text{CO}_2$  (Golterman, 2004; House, 2003; Stumm and Morgan, 1996). This may contribute to the initial removal of DRP from the water column, whereby further adsorption or mineral transformations (e.g., towards hydroxyapatite) may occur (Diaz et al., 1994; Golterman, 1988; Plant and House, 2002). Given the dependence on water-column geochemistry, Ca-based P attenuation is likely a function of catchment geology (Corman et al., 2015; House, 2003; Mulholland et al., 1997). Indeed, most studies focused on Ca-based P attenuation are largely located in catchments with calcareous (i.e., chalk, karst) geology (Cohen et al., 2013; Diaz et al., 1994; House, 1999; Jarvie et al., 2006). Few studies have considered a range of geologies where other abiotic P attenuation mechanisms may diminish the importance of Ca-based P attenuation, particularly sediment P sorption.

Benthic stream sediments can have large potential to adsorb P and thus attenuate P inputs (Froelich, 1988; Haggard and Sharpley, 2007; McDowell, 2015), especially for baseflow conditions where water is given time to contact sediments in the hyporheic zone (Harvey, 2016). Stream sediments provide abundant reactive surfaces for P sorption; notably, clay minerals and metal (i.e., iron and aluminum) oxides are strong reaction sites (Gérard, 2016; Golterman, 2004; Parfitt, 1979). Further, amorphous iron (Fe) oxides, a variable fraction of the total sediment Fe pool (Jan et al., 2013; Parsons et al., 2017), have great affinity for P (Goldberg and Sposito, 1984; Lijklema, 1980) and are the primary reaction sites in many non-calcareous streams (Dupas et al., 2018b; van der Grift et al., 2014; Lewandowski and Nützmann, 2010). This sediment sorption can be readily



examined via intensity of adsorption and the quantity of P already complexed with the sediment. Sorption intensity  
65 measurements often correlate negatively with in-stream DRP (McDaniel et al., 2009; McDowell, 2015; Weigelhofer et al.,  
2018) and positively with stream P uptake metrics (Demars, 2008; Haggard et al., 2005; Jarvie et al., 2005). Concordantly,  
sediments in streams with high P loading (i.e., high sustained DRP concentrations) tend to have diminished sorption ability  
and greater stores of P (Jarvie et al., 2012; McDowell, 2015), particularly in the more labile and redox-sensitive pools  
(Lewandowski and Nützmann, 2010).

70 Therefore, in the present study, we examined P attenuation mechanisms in streams at baseflow via Ca-P geochemistry in the  
water column, stores of sediment P and Fe, and P sorption capacities of sediments. Given that these processes are likely all  
tied to catchment geology and P inputs, we sampled waters and benthic sediments of streams in the Canterbury region, New  
Zealand, covering a variety of geologies, land use, and stream characteristics. We hypothesized that the primary mechanisms  
responsible for P attenuation (and therefore related to DRP concentrations) were Ca-based mineral equilibria in the water  
75 column and sorption with benthic sediments. Further, we hypothesized that amorphous, reactive Fe was a primary controller  
of sediment P sorption, rather than refractory or total Fe pools.

## 2 Materials and methods

### 2.1 Study sites

We sampled 31 streams in the Canterbury region, New Zealand (Fig. 1). The site characteristics are given in Table S1,  
80 according to the River Environment Classification (REC) developed for New Zealand (Snelder and Biggs, 2002). Stream sizes  
were mostly 1<sup>st</sup> to 5<sup>th</sup> order, with some 6<sup>th</sup> and 7<sup>th</sup> order streams ( $n=7$ ), and generally included both low-elevation and  
hilly/mountainous streams. Most of the catchments contained some amount of pastoral land uses (i.e., sheep and dairy farming),  
reflecting the dominant land use in the Canterbury region. In north Canterbury, basins are characterized by quaternary fluvial  
gravels with some underlying sedimentary deposits (e.g., limestone); further south, the plains were formed by river-deposited  
85 erosion and glacial outwash products (by the Rakaia and Waimakariri Rivers), with some intermittent outcrops of greywacke;  
Banks Peninsula is characterized by a basalt volcanic geology (Brown, 2001). Using the scheme provided by the REC,  
catchment geology of the study streams corresponded to alluvium ( $n=15$ ), sedimentary (hard and soft sedimentary;  $n=10$ ), and  
volcanic basic ( $n=6$ ); for presentation and discussion purposes, we grouped the observed data in this paper based on these  
geology classes (see below). Further, we used the REC to distinguish between two prominent sources of flow for the streams  
90 by identifying spring-fed sites ( $n = 8$ ) from the other sites (simply termed here as ‘hill-fed’;  $n = 23$ ).

### 2.2 Sampling procedure

Sediment and stream water samples were collected at each site during baseflow conditions from March to May, 2018 (austral  
late summer/early autumn). We sampled between 1000 and 1600 h to minimize possible diel effects on DRP (Cohen et al.,  
2013; McDowell et al., 2019). Benthic sediments (top 1-3 cm) were collected *in-situ* with a scoop and wet-sieved in the field



95 to <2 mm. The sieved sediment slurry settled after 30 minutes, where excess water was decanted and ~2 kg of wet sediment was stored on ice and later refrigerated in the laboratory (4 °C). Sediment sampling locations were targeted within the stream where surface water interacts with benthic sediments; primarily, riffle beds near the centroid of flow were sampled but depositional areas closer to the bank were sampled at sites where the stream was too deep and fast-flowing for practical sampling.

100 Water grab samples were collected from the centroid of flow via wading (approaching site from downstream) or with an extended pole and bottle. Sample bottles were field-rinsed three times before taking a sample at two-thirds of the stream depth. Two subsamples were filtered in the field (0.45 µm) while another subsample was left unfiltered (all with minimal headspace); all samples were then stored on ice for transport back to the laboratory followed by either freezing (-20 °C; for ion chromatography, ICP-OES, and dissolved Fe as explained below) or refrigeration (4 °C). In addition, we measured dissolved

105 oxygen and temperature at each stream.

### 2.3 Water physicochemical analyses

Upon return to the laboratory, we immediately measured pH and conductivity in the unfiltered stream sample. Alkalinity was measured on the filtered sample within 24 h of collection via Gran's titration method (Gran, 1952), following the protocol of Rounds (2012) with 0.05 M HCl as the titrant. We also measured DRP on the filtered sample within 24 h via the malachite-green method (detection limit of 0.006 mg P L<sup>-1</sup>; Ohno and Zibilske, 1991; D'Angelo et al., 2001) to minimize storage

110 influences (Jarvie et al., 2002). Other analyses on the filtered sample included dissolved anions (F, Cl, SO<sub>4</sub>, NO<sub>3</sub>) via ion chromatography (detection limits range 0.02 to 0.50 mg L<sup>-1</sup>), cations (Al, Ca, Fe, K, Mg, Mn, Na, Zn) via ICP-OES (detection limits approximately 0.002 mg L<sup>-1</sup>), and total dissolved Fe via a ferrozine method (see below); other elements (e.g., some trace metals) were below detection. Total suspended solids (TSS; method 2540D (APHA, 2005)) were low in these streams at

115 baseflow (mean of 7 mg L<sup>-1</sup>), so suspended sediment likely had negligible influence on DRP (data not shown). Blanks and duplicate checks were included in each batch of samples to ensure quality of results.

We modified the ferrozine colorimetric method (Stookey, 1970) developed by Viollier et al. (2000) to measure total dissolved Fe in stream samples and P fractions (below), as it was cost-effective and provided greater sensitivity than ICP-OES for concentrations <0.050 mg Fe L<sup>-1</sup>. Full details are in the supplementary material (S1.3). Briefly, the aliquot reacted with the

120 ferrozine reagent and the reducing agent for 16 h under light conditions (to benefit from photoreduction; Anastácio et al., 2008) before being buffered at pH 9.5 and reading the absorbance at 562 nm. The method detection limit with a 1 cm light path was approximately 0.010 mg Fe L<sup>-1</sup> in solutions and 0.017 mg Fe L<sup>-1</sup> for digests.

### 2.4 Sediment physicochemical analyses

A sediment sample was dried at 104 °C to measure moisture content. Fresh sediment pH was measured in D.I. water at 1:5

125 sediment to solution ratio. We measured two common P sorption indices on fresh sediment: anion storage capacity (ASC; Blakemore et al., 1987) and the Bache-Williams index (BWI; Bache and Williams, 1971) as modified by Burkitt et al. (2002).



Both are single-point isotherms with overnight shaking (16 h) but differ in their conditions. ASC uses solution that is buffered at pH of 4.6 with 1000 mg P L<sup>-1</sup> (1:5 sediment to solution ratio) and expressed as percent removal of P. BWI uses a 0.01 M CaCl<sub>2</sub> solution (no pH buffer) with 1000 mg P kg<sup>-1</sup> sediment added (here, 100 mg P L<sup>-1</sup> at sediment to solution ratio of 1:10) and is expressed as P sorption (mg P kg<sup>-1</sup> sediment) divided by log<sub>10</sub>(c<sub>e</sub>) where c<sub>e</sub> is the remaining equilibrium solution concentration in μg P L<sup>-1</sup>. After centrifuging (2400 g for 15 minutes), the supernatants were analyzed for DRP via the molybdenum-blue method (Murphy and Riley, 1962).

A subsample of sediment was freeze-dried and analyzed for total C and N with a CN elemental analyzer and for total element concentrations with ICP-OES following microwave digestion with nitric acid plus hydrogen peroxide. Additionally, dried sediment samples were sieved to <1 mm and analyzed for particle size distributions via laser-diffraction, which are expressed on a percent volume basis (Eshel et al., 2004); here, we define clays as ≤ 4 μm, silt as > 4 μm and ≤ 62.5 μm, and sands as > 62.5 μm.

## 2.5 Sediment phosphorus fractionation

We began sediment P fractionation within a week of sampling using fresh (not dried) sediments (Simpson et al., 2019) following the scheme of Jan et al. (2015). The primary details of the sequential fractionation are given here and in Table 1; further details are given in the supplementary material (S1). We used 0.5 g d.w. sediment and 10 mL of extractant in each step, in triplicate. The bicarbonate-dithionite (BD) solution (0.1 M NaHCO<sub>3</sub> and 0.1 M Na<sub>2</sub>S<sub>2</sub>O<sub>4</sub>, pH 7.2; BD-I and BD-II fractions) was prepared fresh with de-aerated D.I. water (subject to vacuum for 30 min) and used immediately. The NaOH (I and II) and HCl fractions used 1 M NaOH and 0.5 M HCl, respectively. A 0.5 M NaCl wash step was included after the BD-II and NaOH-II steps to prevent carryover to the next fraction (Condrón and Newman, 2011; Jensen and Thamdrup, 1993). Following the extraction at room temperature with an end-over-end shaker, we centrifuged (10 min at 2400 g) and filtered the extracts (Whatman grade 41). The BD-I and NaOH-I fractions involved 5 min of shaking, immediate centrifuging, decanting, and a further 5 min extraction (i.e., 10 minute total extraction time) as per Jan et al. (2015).

We did not analyze DRP in the BD extracts due to analytical difficulty (Lukkari et al., 2007); however, we suspected little, if any, organic P would contribute to the TP signal since BD primarily targets phosphate associated with reducible metal oxides (Jan et al., 2013; Jensen and Thamdrup, 1993). Although we used a colorimetric method suited for alkaline extracts (He and Honeycutt, 2005), RP concentrations in the NaOH fractions were likely compromised by silicates since the strong alkaline solution solubilizes silica minerals (Lindsay, 1979; Sauer et al., 2006) and silicate produces a molybdenum-blue complex analogous to phosphate (Nagul et al., 2015). However, NaOH-TP values are still valid since digestion removes the silicate interference (Malá and Lagová, 2014; Zhang et al., 1999). Therefore, we restrict our discussion to NaOH-TP. Total P in the BD and NaOH fractions was determined via acid-persulfate autoclave digestion (method 4500-P; APHA, 2005) followed by the molybdenum-blue method (method detection limit of ~0.02 mg P L<sup>-1</sup> for digests). More analytical details are in the supplementary material (S1.2).



In addition to the P in each fraction, we measured total Fe in the BD and NaOH digests with the ferrozine method described above. We examined patterns in Fe and P contents among the BD and NaOH fractions with molar Fe:P ratios. All fractionation data presented in this paper are based on the averages of the laboratory triplicate analyses.

## 2.6 Geochemical equilibria

We examined phosphate mineral equilibria with regard to streamwater chemistry to determine the direction of potential precipitation/dissolution reactions (Pierzynski et al., 2005). We employed the PHREEQC geochemical model (Parkhurst and Appelo, 2013) with the MINTEQA2 version 4 database to calculate mineral saturation indices (SIs) and therefore discuss saturation states with reference to the minerals (Appelo and Postma, 2005). A mineral's SI is defined as  $\log_{10}(IAP/K_{sp})$ , where IAP is the ion activity product measured in solution and  $K_{sp}$  is the mineral's equilibrium solubility constant. A SI  $>0$  and SI  $<0$  indicate super- and subsaturation with respect to the mineral phase. We employ these data to detect if the thermodynamic equilibria favor precipitation reactions as a potential mechanism for DRP removal, but cannot determine what phases actually occur as there may be kinetic limitations (Plant and House, 2002; Stumm and Morgan, 1996). The analytical input data consisted of: stream temperature, pH, total dissolved anions and cations, alkalinity, and DRP. Here, we assumed DRP to be primarily orthophosphate. Since these streams were above or near oxygen saturation at time of sampling, we assumed that Fe was in an oxidized state (Fe(III)).

## 2.7 Data and statistical methods

Two sites in the sedimentary class – both at pristine, forested headwaters – had DRP concentrations below our detection limits. To mitigate potential bias, we inserted reference DRP values based on previous analyses for streams under the same classification within the REC (McDowell et al., 2013). Additionally, through exploratory analyses, we found it necessary to remove data with a spring-fed source of flow as a confounding variable when modelling DRP (see below). We hypothesized that the spring-fed streams had greatly diminished hyporheic exchange – thus limiting the interaction between sediment reaction sites and the water column. This limitation could be due to 1) accumulation of fine, silty sediments which restricted hydraulic conductivity (Aubeneau et al., 2014; Packman and Salehin, 2003; Weigelhofer et al., 2018), 2) low-gradients which limited hydrodynamic forces at the streambed (Boano et al., 2014), and 3) the likely presence of groundwater inputs along the reach, which are known to limit hyporheic exchange flows (Azizian et al., 2017).

We summarized differences between the stream and sediment variables (physico- and geochemical) between the three geology classes with nonparametric tests (Hollander et al., 2013). We first tested the null hypothesis ( $H_0$ ) that the locations of the group-wise distributions were equal via the Kruskal-Wallis test; if  $H_0$  was rejected, we then constructed multiple comparisons with rank statistics, adjusting for simultaneous inferences (Konietschke et al., 2012, 2015). Additionally, Spearman correlations were used to describe relationships between variables of interest. We explored the sediment-P attenuation mechanism in streams by fitting simple predictive models (Shmueli, 2010); we used robust linear models (“rlm” function in MASS package; Venables and Ripley, 2002) to model DRP and sediment P sorption (see supplementary material; S2). All tests were performed



at 95% confidence and all analyses were conducted in R (version 3.5.2; R Core Team, 2018). The data can be found at Figshare (<https://figshare.com/s/718226c7f1940d631755>).

### 3 Results

#### 3.1 Stream water chemistry and mineral equilibria

195 Stream physicochemistry at the time of sampling is summarized in Table 2. The streams ranged from low to moderate alkalinity (16.7 to 88.8 mg CaCO<sub>3</sub> L<sup>-1</sup>, mean of 42.7 mg CaCO<sub>3</sub> L<sup>-1</sup>) and mean conductivity was 143 μS cm<sup>-1</sup>. For the time of sampling (generally, 1000 to 1600 h), pH averaged 7.44 (6.43 to 7.93). Dissolved reactive P varied among geology classes with the lowest median DRP concentration in sedimentary, followed by alluvium, and then by volcanic basic (5.0, 7.4, and 27.7 μg P L<sup>-1</sup>, respectively).

200 Stream geochemical equilibria modelling with PHREEQC was used to examine important mineral phases in the water column (Fig. 2). Stable, yet kinetically slow-to-form, Al and Fe minerals such as gibbsite and goethite were supersaturated in the water column; amorphous Al species (Al(OH)<sub>3</sub>(am)) were subsaturated. The most reactive Fe species studied here, ferrihydrite (Fe(OH)<sub>3</sub>(am)), was supersaturated (overall mean SI 1.9 ± 0.6), particularly over volcanic basic geologies (mean SI 2.9 ± 0.2). We note that ferrihydrite SI correlated with log-activity of HPO<sub>4</sub><sup>2-</sup> (ρ = 0.71, *p* < 0.001). Further, CaCO<sub>3</sub> precipitation was not  
205 favorable (SI range of -2.1 to -0.08). Therefore, for these grab samples, CaCO<sub>3</sub> co-precipitation of phosphate was not a likely mechanism.

Phosphate mineral solubilities were also investigated. The activities of phosphate and Fe/Al were too low to precipitate any P minerals from the water column in these streams (e.g., strengite; Fig. 2). For Ca-phosphate minerals, the less thermodynamically stable phases (e.g., CaHPO<sub>4</sub>·(H<sub>2</sub>O)<sub>2</sub>) were sub-saturated in all samples. However, several streams showed  
210 saturation to slight super-saturation with respect to hydroxylapatite; log-activity of HPO<sub>4</sub><sup>2-</sup> is plotted against a function of Ca<sup>2+</sup> and H<sup>+</sup> activities with reference to the standard solubility curve of hydroxylapatite in Fig. 3. All three geologies had some waters with positive hydroxylapatite SIs but, notably, the saturation appears to not extend significantly past the hydroxylapatite solubility curve (max SI of 1.7). We noted no other geochemically significant relationships for other mineral SIs (Fig. S1) or ion log-activities (Fig. S2). Given that most phosphorous minerals of interest were sub-saturated in the water column, and that  
215 hydroxylapatite likely requires greater SI values before actively precipitating (see discussion below), mineral precipitation does not seem a significant mechanism for P removal in these streams.

#### 3.2 General stream sediment physicochemistry

Physicochemical characteristics of the benthic sediments are summarized in Table 3. The sediments were largely neutral (mean pH of 7.10). The fine sediments sampled in this survey were predominantly sandy (mean sand content of 84%), although five  
220 alluvium sites and two volcanic basic sites had less than 80% sand content (silt + clay content range from 21 to 92%). Sediments from spring-fed streams were much finer (D<sub>50</sub> of 171 ± 172 μm) than those in hill-fed streams (597 ± 172 μm). The sediments



were relatively low in total C (overall median of  $3.0 \text{ g C kg}^{-1}$ ) except for the spring sites (median of  $20 \text{ g C kg}^{-1}$ ). Owing to the different geological origins, the volcanic basic sediments were enriched with Al, Fe, Mn, and P in comparison to the sedimentary and alluvium sediments.

### 225 3.3 Stream sediment phosphorus and iron fractionation

#### 3.3.1 Phosphorus fractionation

Sediment P concentration fractionated according to the procedure by Jan et al. (2015) varied considerably by the catchment geology (Fig. 4). The most labile pool,  $\text{H}_2\text{O-P}$ , was relatively high in the volcanic basic sediments (mean  $\pm$  SD;  $3.84 \pm 3.76 \text{ mg P kg}^{-1}$ ) and alluvium sediments ( $1.82 \pm 1.41 \text{ mg P kg}^{-1}$ ), but lower for sedimentary sites ( $0.44 \pm 0.08 \text{ mg P kg}^{-1}$ ; Table 4).

230 Both reductively-soluble sediment P pools, BD-I and BD-II, were enriched in alluvium and volcanic basic sediments in comparison to sedimentary sites, with total BD-extractable P (BD-I plus BD-II) of  $84.3 \pm 84.1$ ,  $77.6 \pm 26.7$ , and  $6.60 \pm 3.03 \text{ mg P kg}^{-1}$ , respectively. The mean proportion of the reductively-soluble sediment P pool attributed to amorphous Fe oxides (BD-I), rather than crystalline Fe oxides (BD-II), was 62% in alluvium sediments but evenly distributed in volcanic basic sediments (49%). Both BD-I and BD-II P fractions correlated with fines (clays plus silts) concentration (respectively,  $\rho = 0.89$  and  $0.84$ ,  $p < 0.001$  for both tests; Fig. S3). Further, the labile P pools of  $\text{H}_2\text{O-P}$  and BD-I P together comprised only 0.5 to 21% of total P, with means of  $1.0 \pm 0.5$ ,  $8.2 \pm 6.7$ , and  $2.1 \pm 1.4\%$  for the sedimentary, alluvium, and volcanic basic geologies, respectively.

The NaOH-extractable P pool averaged  $34.3 \pm 10.7$ ,  $91.8 \pm 84.7$ , and  $518 \pm 329 \text{ mg P kg}^{-1}$  for sediments from the sedimentary, alluvium, and volcanic basic geologies, respectively. The more labile NaOH fraction (NaOH-I) made up the majority of the total NaOH-extractable P pool (67-71% on average). Total NaOH-extractable P correlated with Al content ( $\rho = 0.47$ ,  $p = 0.008$ ), but no other relationships (e.g., with total C) were evident. The least available sediment P pool analyzed, HCl-P, averaged  $452 (\pm 161)$ ,  $337 (\pm 163)$ , and  $1373 (\pm 572) \text{ mg P kg}^{-1}$  for sites in the sedimentary, alluvium, and volcanic basic geologies, respectively. As expected, HCl-P correlated strongly with Ca ( $\rho = 0.84$ ,  $p < 0.001$ ) and Mg content ( $\rho = 0.71$ ,  $p < 0.001$ ) since this fraction is dominated by primary mineral P.

245 In-stream DRP correlated well with both  $\text{H}_2\text{O-P}$  and the sum of  $\text{H}_2\text{O-P}$  and BD-I P (hereafter, labile P; Fig. 5). Using sediment P pools as the primary predictors for DRP in hill-fed streams (Table S2), the best-fit linear model employed geology and  $\text{H}_2\text{O-P}$  (RMSE =  $3.93 \mu\text{g P L}^{-1}$ ), with a slope (95% C.I.) of  $2.62 (1.58 \text{ to } 3.66) \mu\text{g P L}^{-1}$  per  $\text{mg P kg}^{-1}$  for  $\text{H}_2\text{O-P}$ .

#### 3.3.2 Iron fractionation

In addition to P, we measured Fe in selected extracts of the P fractionation scheme (Fig. 6). Although total Fe is similar between alluvium and sedimentary sites (means of  $22.0$  and  $23.4 \text{ g Fe kg}^{-1}$ ; Table 3), reactive Fe pools varied markedly within and between all catchment geologies (Table 4). Total BD-extractable Fe was  $2280 (\pm 2200)$ ,  $700 (\pm 242)$ , and  $7710 (\pm 2120) \text{ mg Fe kg}^{-1}$  for the alluvium, sedimentary, and volcanic basic sites, respectively. On average, the amorphous Fe pool made up 52,



38, and 34% of the BD-extractable Fe in alluvium, sedimentary, and volcanic basic sediments. The BD-extractable pools of Fe correlated with percent fines (Fig. S4), where Spearman  $\rho$  was 0.87 ( $p < 0.001$ ) and 0.79 ( $p < 0.001$ ) for BD-I and BD-II, respectively. The Fe extracted by NaOH was at least one order of magnitude less than BD-extractable Fe for each geology (totals of 59 to 250 mg Fe kg<sup>-1</sup>); NaOH-I Fe related to percent fines ( $\rho = 0.77$ ,  $p < 0.001$ ) and total C ( $\rho = 0.75$ ,  $p < 0.001$ ), which is likely due to release of Fe complexed with organic matter during extraction. In general, the BD- and NaOH-extractable Fe scaled with total Fe ( $\rho = 0.45$  ( $p = 0.012$ ) and  $\rho = 0.39$  ( $p = 0.033$ ), respectively). However, reactive Fe contributed only a minor portion of total Fe in these sediments ( $8.6 \pm 7.2\%$  and  $0.6 \pm 0.8\%$  for total BD- and NaOH-extractable Fe, respectively; Fig. 6).

### 3.3.3 Fe:P ratios in sediments

Molar Fe:P in pools of sediment P varied depending on the pool and the catchment geology (Table 4, Fig. S5). In general, Fe:P ratios were much lower for the NaOH fractions (approximately 0.25 to 3 mol Fe mol P<sup>-1</sup>) than for other fractions (>13 mol Fe mol P<sup>-1</sup>), likely due to little surface reactive Fe left after BD extraction while containing P bound with constituents other than Fe. A paired Wilcoxon signed-rank test on Fe:P ratios in the BD fractions indicated that BD-II Fe:P is, on average, 25.6 (95% C.I., 14.4 to 36.1) mol Fe mol P<sup>-1</sup> greater than BD-I Fe:P. However, Fe:P ratios for either BD-I or BD-II fractions did not improve linear model fits for either DRP or ASC (data not shown). For the BD (I and II) fractions, median Fe:P was less in alluvium sediments (15.5 and 19.9 mol Fe mol P<sup>-1</sup>) compared to both sedimentary (36.4 and 80.7 mol Fe mol P<sup>-1</sup>) and volcanic-basic sediments (39.1 and 85.8 mol Fe mol P<sup>-1</sup>).

### 3.4 Stream sediment phosphorus sorption

Sediment P sorption metrics are summarized in Table 4. Although ASC (a measure of P retention at low pH) and BWI (P retention at neutral pH and controlled Ca concentration) differ in how P sorption potential is determined, a similar pattern was apparent in both variables for the three sampled geologies. Given the widespread use of ASC in soil classification (and management) in New Zealand (Saunders, 1965), we focus on ASC for brevity. The sedimentary samples had lower ASC ( $10.2 \pm 5.6\%$ ) than either alluvium ( $33.6 \pm 26.9\%$ ) or volcanic basic sediments ( $49.4 \pm 11.1\%$ ). There was no clear relationship between ASC and sediment Fe:P ratios (Fig. S6), while ASC was correlated with BD-I ( $\rho = 0.77$ ,  $p < 0.001$ ), BD-II ( $\rho = 0.65$ ,  $p < 0.001$ ), and total Fe ( $\rho = 0.55$ ,  $p = 0.002$ ) pools (Fig. 7).

More refractory pools of Fe were less predictive of ASC than BD-I Fe (Fig. 7). While ASC for the refractory Fe pools tended to cluster according to geology and stream source of flow, ASC varied linearly as a function of BD-I Fe (all data), which we illustrate with a linear modelling exercise, summarized in Table S3. The simple model of only BD-I Fe had the lowest AIC and the lowest RMSE (9.2 %); the estimated slope for BD-I Fe was 0.0174 (95% C.I., 0.0152 to 0.0197) % per mg Fe kg<sup>-1</sup>. Additionally, while adding catchment geology did not improve the model fit for BD-I Fe, both the BD-II and total Fe models included this term for their respective optimal models. Thus, BD-I Fe alone predicted ASC optimally and captured the variance otherwise provided by geology or refractory Fe to the lesser models.



285 Contrary to our expectations, sediments with greater sorption potential positively correlated with in-stream DRP (Fig. 8), but  
only for the case of hill-fed streams. In addition to the linear models fitted with the labile P fractions above, we used ASC as  
a predictor of DRP (Table S2) – again, we excluded spring-fed sites as a confounding variable. Using ASC alone gave similar  
performance (RMSE of  $4.44 \mu\text{g P L}^{-1}$ ) as the models with terms for geology and the labile P fractions, but with less model  
degrees of freedom. Overall, the best linear model for DRP employed ASC and  $\text{H}_2\text{O-P}$  (RMSE of  $4.38 \mu\text{g P L}^{-1}$ ), with slopes  
290 of  $2.03 (1.22 \text{ to } 2.83) \mu\text{g P L}^{-1}$  per  $\text{mg H}_2\text{O-P kg}^{-1}$  and  $0.325 (0.218 \text{ to } 0.431) \mu\text{g P L}^{-1}$  per ASC %.

#### 4 Discussion

Phosphorus in streams does not travel as a conservative solute. Our data suggests that bioavailable P, i.e., DRP and labile  
sediment P fractions, in these streams is likely to be modified by two principal factors: 1) reactive Fe content as derived from  
both geology and in-stream Fe cycling, and 2) the exchange between sediment porewaters and the water column (i.e., hyporheic  
295 exchange) as governed by hydraulic forces and sediment particle size distribution. We summarize our lines of evidence to  
support this hypothesis below.

##### 4.1 Stream water-column geochemistry and dissolved reactive phosphorus

Catchment geology is a primary control on the geochemical composition of stream water (Bluth and Kump, 1994; Stumm and  
Morgan, 1996), and our results suggest that the Ca-based mechanisms for P removal were insignificant in our streams. Among  
300 the geochemical equilibria affecting phosphate in solution, phosphate-minerals rarely had the thermodynamic potential to form  
in these waters. The most stable phosphate mineral, hydroxylapatite, showed some cases of near-saturation ( $\text{SI} \approx 0$ ; Fig. 3).  
However, empirical research has suggested that the required supersaturation for hydroxylapatite to significantly precipitate  
from solution is much higher (reported SI from 3 to 10; House, 1999; Plant and House, 2002; Sørensen et al., 2011). Therefore,  
hydroxylapatite and other phosphate-mineral precipitation seems, at best, a secondary mechanism for P removal in these  
305 streams. In contrast, streams with greater Ca concentrations (e.g.,  $>100 \text{ mg Ca L}^{-1}$ ) and pH ( $>8$ ) will likely be more conducive  
for Ca-P mineral precipitation (Diaz et al., 1994). It is striking that some streams approach, but do not significantly extend  
beyond, the hydroxylapatite solubility curve, which could suggest a role for hydroxylapatite equilibrium. However, stream  
solution chemistry is more complex than ideal solutions modelled by PHREEQC, where even the solubility constant for  
hydroxylapatite is subject to considerable uncertainty (Golterman, 2004). In addition, other phosphate-minerals (e.g., various  
310 Al and Fe based phosphate-minerals) are unlikely to contribute to phosphate activity in the water column, but may be more  
important in some subsurface environments (e.g., Denver et al., 2010; Rothe et al., 2014).  
Since, calcite co-precipitates with phosphate (Golterman, 2004; House, 2003), periods of calcite precipitation in streams may  
provide an opportunity for phosphate removal, particularly in low-phosphate systems (Machesky et al., 2010; Plant and House,  
2002; Sørensen et al., 2011). House (1999) suggested that calcite precipitation in streams becomes significant near  $\text{SI} \approx 1$ . In the  
315 present study, however, we only observed negative SI's for calcite (Fig. 2). Our study design was more likely to capture the



upper extent of calcite SI variability since: 1) calcite saturation peaks during the day when photosynthesis depletes  $\text{CO}_2(\text{g})$  and increases pH (Nimick et al., 2011; Stets et al., 2017) and 2) calcite solubility decreases with greater temperatures during the day (Stumm and Morgan, 1996). It is likely that our study streams were not alkaline enough for significant calcite interactions (here, median alkalinities of 38.2 to 42.1, maximum of  $88.8 \text{ mg L}^{-1}$  as  $\text{CaCO}_3$ ; maximum pH of 7.93; Table 2) since streams  
320 that reach a calcite  $\text{SI} \geq 1$  typically have alkalinity  $>100 \text{ mg L}^{-1}$  as  $\text{CaCO}_3$  and sustain  $\text{pH} > 8$  (Corman et al., 2015; Neal et al., 2002; Nimick et al., 2011; Stets et al., 2017). Hence, we rule out calcite-phosphate co-precipitation as a significant mechanism for DRP removal in these streams.

The removal of P in streams via Ca-P mechanisms is frequently documented (Burns et al., 2015; Cohen et al., 2013; Jarvie et al., 2006), but such studies are located in catchments dominated by carbonaceous/karst geologies. Since many streams suffering  
325 from P pollution may not have such ‘self-cleansing’ mechanisms available, knowledge of other processes for P attenuation are critical for understanding P transport.

Aside from Ca-based solution geochemistry, an unexpected observation from this study was the supersaturation of ferrihydrite and its relationship with  $\text{HPO}_4^{2-}$  activity (Fig. S1). Ferric iron is largely insoluble in most stream conditions (oxygenated water and pH near or above neutral) and Fe(II) would presumably be associated only with reducing zones within the stream corridor  
330 (Stumm and Sulzberger, 1992), thus positive ferrihydrite SI seems implausible. Fox (1988) explained the problem that, in most streams, dissolved Fe is overestimated because common filtration methods (i.e.,  $0.45 \mu\text{m}$  filters) fail to remove colloidal Fe species (Baken et al., 2016b; van der Grift et al., 2014). Our apparent supersaturation with respect to ferrihydrite is within the range of previously observed over-estimates (SI up to 5 in most cases; Fox, 1988) and is a limitation of our dataset. However, the positive relation between ferrihydrite SI and DRP may indirectly point towards evidence of colloidal Fe species carrying  
335 sorbed phosphate and should be investigated in future research.

#### 4.2 Amount and form of sediment phosphorus depends on geology

Given the enormous amounts of sediment that stream networks retain and the long timescales for its transit (Czuba et al., 2017; Wohl, 2015), P bound in benthic sediments represents a crucial component of legacy P. However, we found that most sediment P was unlikely to be bioavailable in our study streams (Fig. 4). Taking  $\text{H}_2\text{O}$  and BD-I extractable P (labile P) as potentially  
340 bioavailable in lotic systems and definitely available in receiving lentic systems (e.g., lakes; Golterman, 2004; Jan et al., 2015; Jensen and Thamdrup, 1993; Monbet et al., 2010), sediment labile P was generally  $<10\%$  of total P (maximum of 21% of total P), but varied with geology. Although small, these pools are highly reactive under baseflow and may be subjected to microbial turnover (McDowell, 2003), exchange with porewaters via desorption or reductive dissolution (Lewandowski and Nützmann, 2010; Parsons et al., 2017; Zak et al., 2006), and potentially to P-scavenging periphyton mats (Wood et al., 2015).

#### 345 4.3 Amorphous iron content determines sediment phosphorus sorption capacity

Benthic sediment Fe has long been thought to provide much of the reactivity for P in streams (Danen-Louwerse et al., 1993; Froelich, 1988; Wauchope and McDowell, 1984). Therefore, we selected a fractionation scheme to target the responsible



fractions of Fe. To our knowledge, our study is the first application of the sediment P fractionation scheme developed by Jan et al. (2015) to stream sediments. The motivation behind this fractionation scheme is that, in the absence of precipitation mechanisms, the more soluble, amorphous forms of Fe and Al oxides are the ones responsible for P retention and possible release (Jan et al., 2013, 2015; Postma, 1993). With this fractionation, we found large differences between catchment geologies and substrate texture (coarse sediments in hill-fed streams vs. silty sediments in spring-fed streams) in the amounts of reactive Fe (both BD-I and BD-II Fe) and its associated P, while total Fe was much less variable (Fig. 4 and Fig. 6). Further, BD-I Fe alone predicted sediment P sorption potential, as opposed to the more crystalline (BD-II) or refractory (total) Fe pools (Fig. 7, Table S3). Hence, we focus our discussion around BD-I Fe and its implications for stream P transport.

The first BD step efficiently targets surface-reactive, amorphous Fe oxides, while the second BD step extracts more-crystalline, less reactive Fe oxides (Jan et al., 2015). This geochemical difference was evident in the Fe:P ratios (Table 4), where mean BD-I Fe:P ratios (varying with geology from  $18.3 \pm 9.9$  to  $65.0 \pm 66.9$ ) were significantly lower than BD-II Fe:P ( $31.6 \pm 25.1$  to  $99.2 \pm 61$ ), owing to the greater affinity for P in the amorphous fraction. Pure Fe-P minerals would have much lower Fe:P ratios (e.g., 1 for  $\text{FePO}_4$ ); laboratory studies have observed molar Fe:P ratios of approximately 2 to 5 for P incorporated into Fe oxides during precipitation (Deng and Stumm, 1994; Senn et al., 2015) or adsorbed onto fresh Fe oxide precipitants (Lijklema, 1980). In their study, Senn et al. (2015) report that Fe(III) precipitants in environmental conditions similar to that within many streams and hyporheic zones (circumneutral pH, varying amounts of Ca,  $\text{PO}_4$ , and silicate) are a complex mixture of basic (Ca-)  $\text{FePO}_4$ , ferrihydrite-type, and poorly crystalline lepidocrocite/goethite precipitants. This mixture of Fe(III) precipitants with varying stoichiometries and phosphate sorption capacities may explain the wide variance we observed in the BD-I Fe:P ratios. For the BD-II fraction, Fe:P may be related to the weathering status of the parent sediment material (Lair et al., 2009), as more crystalline Fe oxides become less sorptive for P. Total Fe:P is less meaningful (Jan et al., 2013), due to the varying contributions of Fe oxides to the total Fe and of other pools of P (e.g., NaOH-extractable P) to the total P (Hoffman et al., 2009; Machesky et al., 2010). Here, the contribution of BD-extractable Fe to the total Fe was generally  $<10\%$ , indicating that much sediment Fe can be unimportant to in-stream P cycling.

While the Fe:P ratios differentiated pools of Fe according to their geochemical affinity for P (BD-I vs. BD-II), Fe:P ratios were poor predictors of sediment P sorption, likely due to the variable composition of Fe species present in these pools (Herndon et al., 2019; Senn et al., 2015). This result contrasts with previous notions that Fe:P indicates available sorption sites (Coelho et al., 2004; Jensen et al., 1992; Kronvang et al., 2009). Rather than the Fe:P ratio, our data suggests that the mass of BD-I Fe alone was largely responsible for sediment P sorption (Fig. 7, Table S3). This result was consistent regardless of sediment texture, source of flow, or catchment geology. Notwithstanding the contribution of Al oxides to P sorption (Danan-Louwerse et al., 1993; Mendes et al., 2018), reactive Fe species (defined by varying methodologies) are strong predictors of P sorption in a variety of aquatic environments (Machesky et al., 2010; Zhang and Huang, 2007; Zhou et al., 2005). For example, Marton and Roberts (2014) and Herndon et al. (2019) found that the Bache-Williams index (BWI) was predicted by amorphous or reactive Fe oxide contents in peat, tundra, and marsh soils; these observations are matched by our findings in benthic stream



sediments (Fig. 7). While these environments differ substantially, a similar theme is apparent regarding Fe-P relationships: where redox interfaces generate amorphous Fe oxides, there is a greater potential for P adsorption.

#### 4.4 The ability for sediments to influence dissolved reactive phosphorus depends on reactivity and connectivity

The above discussion infers that reactive Fe oxides are efficient traps for P but in reality – due to the advective nature of the hyporheic zone and the high spatiotemporal variation in biogeochemistry – the Fe oxides themselves are likely transient (van der Grift et al., 2014; Runkel et al., 1999; Smolders et al., 2017). Our study suggests that DRP paradoxically tends to increase with P sorption potential (Fig. 8), but only for the hill-fed streams. We suspect that, given the P sorption potential in these streams was driven by amorphous Fe oxides (Fig. 7), the dynamics of Fe cycling may be coupled with DRP through: 1) dynamic precipitation and dissolution of Fe oxides and their bound P (Rhoton et al., 2002; Runkel et al., 1999; Smolders et al., 2017) and 2) the generation of Fe colloids at redox interfaces bearing P and elevating DRP (Baken et al., 2016a; Briggs et al., 2015; Gottselig et al., 2017; Ren and Packman, 2005). Both of these mechanisms are constrained for streams with little hyporheic exchange (e.g., the spring-fed streams in the present study; Boano et al., 2014). While we have indications of the former (Fig. 7 and Fig. 8) and latter (ferrihydrite SI correlation with  $\text{HPO}_4^{2-}$  activity; Fig. S1) hypotheses, it is beyond the scope of our study to discuss these meaningfully.

Further research is needed to link the abiotic P exchange mechanisms we have discussed to the spatiotemporal DRP signal observed in the water column. While stream sediments are well-known to provide reaction sites for P, little has been done to link these reaction sites in streams to P cycling in a mechanistic manner, i.e., by connecting these zones of reactivity to hydrological transport (Boano et al., 2014). We suggest that future research on stream P cycling avoids mono-causal interpretations (Kalbitz et al., 2017), and incorporates the multiple mechanisms – both biotic and abiotic – where relevant.

## 5 Conclusions

Water-column and sediment biogeochemistry changes with catchment geology in ways critical to P cycling. Low to moderate alkalinity (i.e.,  $<100 \text{ mg L}^{-1}$  as  $\text{CaCO}_3$ ) streams had little potential to remove P via Ca-based (co-)precipitation mechanisms, making interactions with benthic sediments more important. We found sediment P sorption mechanisms captured within labile sediment P fractions ( $\text{H}_2\text{O}$  and BD-I extractable P) were likely linked to reactive Fe pools that comprised minor proportions of the total Fe content. The amount of this labile sediment P was predominantly driven by the catchment geology. However, the data also suggested that labile P co-varied with DRP where hyporheic exchange likely mediated the interaction between the water column and porewaters in hill-fed streams, whose sediments were more permeable than those in spring-fed streams. Both geology and hyporheic exchange are integral to the attenuation of P in streams and, hence, will need to be accounted for if baseflow DRP concentrations are to be predicted and managed.



#### 410 **Data availability**

The data reported here are available at Figshare (<https://figshare.com/s/718226c7f1940d631755>). The REC geodatabase is available through the New Zealand Ministry for the Environment (<https://data.mfe.govt.nz/data/>).

#### **Author contribution**

Conceptualization: ZS and RM with support from LM. Funding acquisition: RM. Resources & supervision: RM and LC.  
415 Methodology: ZS, RM, and LC. Formal analysis: ZS with support from RM. Investigation, visualization & original draft: ZS.  
All authors contributed to the review and final draft.

#### **Competing interests**

The authors declare that they have no conflict of interest.

#### **Acknowledgements**

420 We thank Julie Clark at University of Otago for analyzing sediments for particle size distributions; Lincoln University technical  
staff for providing laboratory needs and some analyses, particularly Roger Cresswell, Lynne Clucas, Leanne Hassall, Vicky  
Zhang, and Shiv Pokhrel; Florencia De Lucca Agrelo for field and lab assistance; Marion Des Roseaux, Yuan Li, David Rex,  
and Tihana Vujinovic for occasional support; and the Our Land and Water National Science Challenge for funding the study  
(contract C10X1507 from the Ministry of Business, Innovation and Employment). This manuscript benefitted from review by  
425 Andrea Leptin.



## References

- 430 Anastácio, A. S., Harris, B., Yoo, H. I., Fabris, J. D. and Stucki, J. W.: Limitations of the ferrozine method for quantitative assay of mineral systems for ferrous and total iron, *Geochim. Cosmochim. Acta*, 72(20), 5001–5008, doi:10.1016/j.gca.2008.07.009, 2008.
- APHA: Standard Methods for the Examination of Water and Wastewater, 21st Edition., American Public Health Association., 2005.
- 435 Appelo, C. A. J. and Postma, D.: *Geochemistry, groundwater and pollution*, 2nd ed., A.A. Balkema Publishers, Leiden, The Netherlands., 2005.
- Aubeneau, A. F., Hanrahan, B., Bolster, D. and Tank, J. L.: Substrate size and heterogeneity control anomalous transport in small streams, *Geophys. Res. Lett.*, 41(23), 8335–8341, doi:10.1002/2014GL061838, 2014.
- Azizian, M., Boano, F., Cook, P. L. M., Detwiler, R. L., Rippey, M. A. and Grant, S. B.: Ambient groundwater flow diminishes nitrate processing in the hyporheic zone of streams, *Water Resour. Res.*, 53, doi:10.1002/2016WR020048.Received, 2017.
- 440 Bache, B. and Williams, E.: A phosphate sorption index for soil, *Eur. J. Soil Sci.*, 22(3), 289–301, doi:10.1111/j.1365-2389.1971.tb01617.x, 1971.
- Baken, S., Regelink, I. C., Comans, R. N. J., Smolders, E. and Koopmans, G. F.: Iron-rich colloids as carriers of phosphorus in streams: A field-flow fractionation study, *Water Res.*, 99, 83–90, doi:10.1016/j.watres.2016.04.060, 2016a.
- 445 Baken, S., Moens, C., van der Grift, B. and Smolders, E.: Phosphate binding by natural iron-rich colloids in streams, *Water Res.*, 98, 326–333, doi:10.1016/j.watres.2016.04.032, 2016b.
- Biggs, B. J. F.: Eutrophication of streams and rivers: dissolved nutrient-chlorophyll relationships for benthic algae, *J. N. Am. Benthol. Soc.*, 19(1), 17–31, doi:10.2307/1468279, 2000.
- Blakemore, L. C., Searle, P. L. and Daly, B. K.: *Methods for chemical analysis of soils*, NZ Soil Bureau Scientific Report 80., 1987.
- 450 Bluth, G. J. S. and Kump, L. R.: Lithologic and climatologic controls of river chemistry, *Geochim. Cosmochim. Acta*, 58(10), 2341–2359, doi:10.1016/0016-7037(94)90015-9, 1994.
- Boano, F., Harvey, J. W., Marion, A., Packman, A. I., Revelli, R., Ridolfi, L. and Wörman, A.: Hyporheic flow and transport processes: Mechanisms, models, and biogeochemical implications, *Rev. Geophys.*, 52, 603–679, doi:10.1002/2012RG000417.Received, 2014.
- 455 Briggs, M. A., Day-Lewis, F. D., Zarnetske, J. P. and Harvey, J. W.: A physical explanation for the development of redox microzones in hyporheic flow, *Geophys. Res. Lett.*, 42(11), 4402–4410, doi:10.1002/2015GL064200, 2015.
- Brown, L. J.: Canterbury, in *Groundwaters of New Zealand*, pp. 441–459, New Zealand Hydrological Society Inc., Wellington, New Zealand., 2001.
- 460 Burkitt, L. L., Moody, P. W., Gourley, C. J. P. and Hannah, M. C.: A simple phosphorus buffering index for Australian soils, *Soil Res.*, 40(3), 497–513, doi:10.1071/sr01050, 2002.



- Burns, E. E., Comber, S., Blake, W., Goddard, R. and Couldrick, L.: Determining riverine sediment storage mechanisms of biologically reactive phosphorus in situ using DGT, *Environ Sci Pollut Res*, 22(13), 9816–9828, doi:10.1007/s11356-015-4109-3, 2015.
- 465 Coelho, J. P., Flindt, M. R., Jensen, H. S., Lillebø, A. I. and Pardal, M. A.: Phosphorus speciation and availability in intertidal sediments of a temperate estuary: relation to eutrophication and annual P-fluxes, *Estuarine Coastal Shelf Sci.*, 61(4), 583–590, doi:10.1016/j.ecss.2004.07.001, 2004.
- Cohen, M. J., Kurz, M. J., Heffernan, J. B., Martin, J. B., Douglass, R. L., Foster, C. R. and Thomas, R. G.: Diel phosphorus variation and the stoichiometry of ecosystem metabolism in a large spring-fed river, *Ecol. Monogr.*, 83(2), 155–176, doi:10.1890/12-1497.1, 2013.
- 470 Condron, L. M. and Newman, S.: Revisiting the fundamentals of phosphorus fractionation of sediments and soils, *J Soils Sediments*, 11(5), 830–840, doi:10.1007/s11368-011-0363-2, 2011.
- Corman, J. R., Moody, E. K. and Elser, J. J.: Stoichiometric impact of calcium carbonate deposition on nitrogen and phosphorus supplies in three montane streams, *Biogeochemistry*, 126(3), 285–300, doi:10.1007/s10533-015-0156-6, 2015.
- 475 Czuba, J. A., Foufoula-Georgiou, E., Gran, K. B., Belmont, P. and Wilcock, P. R.: Interplay between spatially-explicit sediment sourcing, hierarchical river-network structure, and in-channel bed-material sediment transport and storage dynamics, *J. Geophys. Res. Earth Surf.*, 1–31, doi:10.1002/2016JF003965, 2017.
- Danen-Louwerse, H., Lijklema, L. and Coenraats, M.: Iron content of sediment and phosphate adsorption properties, *Hydrobiol.*, 253(1), 311–317, 1993.
- 480 D’Angelo, E., Crutchfield, J. and Vandiviere, M.: Rapid, sensitive, microscale determination of phosphate in water and soil, *J. Environ. Qual.*, 30(6), 2206–2209, doi:10.2134/jeq2001.2206, 2001.
- Davies, J.-M. and Bothwell, M. L.: Responses of lotic periphyton to pulses of phosphorus: P-flux controlled growth rate, *Freshwater Biol.*, 57(12), 2602–2612, doi:10.1111/fwb.12032, 2012.
- Demars, B. O. L.: Whole-stream phosphorus cycling: Testing methods to assess the effect of saturation of sorption capacity on nutrient uptake length measurements, *Water Res.*, 42(10–11), 2507–2516, doi:10.1016/j.watres.2008.02.010, 2008.
- 485 Deng, Y. and Stumm, W.: Reactivity of aquatic iron(III) oxyhydroxides—implications for redox cycling of iron in natural waters, *Appl. Geochem.*, 9(1), 23–36, doi:10.1016/0883-2927(94)90049-3, 1994.
- Denver, J. M., Cravotta, C. A., Ator, S. W. and Lindsey, B. D.: Contributions of phosphorus from groundwater to streams in the Piedmont, Blue Ridge, and Valley and Ridge physiographic provinces, eastern United States, U.S. Geological Survey, Reston, Va., 2010.
- 490 Diaz, O. A., Reddy, K. R. and Moore, P. A.: Solubility of inorganic phosphorus in stream water as influenced by pH and calcium concentration, *Water Res.*, 28(8), 1755–1763, doi:10.1016/0043-1354(94)90248-8, 1994.
- Dupas, R., Minaudo, C., Gruau, G., Ruiz, L. and Gascuel-Oudou, C.: Multidecadal trajectory of riverine nitrogen and phosphorus dynamics in rural catchments, *Water Resour. Res.*, 54(8), 5327–5340, doi:10.1029/2018WR022905, 2018a.
- 495 Dupas, R., Tittel, J., Jordan, P., Musolff, A. and Rode, M.: Non-domestic phosphorus release in rivers during low-flow: Mechanisms and implications for sources identification, *J. Hydrol.*, 560, 141–149, doi:10.1016/j.jhydrol.2018.03.023, 2018b.



- Ensign, S. H. and Doyle, M. W.: Nutrient spiraling in streams and river networks, *J. Geophys. Res. Biogeosci.*, 111(G4), doi:10.1029/2005JG000114, 2006.
- Eshel, G., Levy, G. J., Mingelgrin, U. and Singer, M. J.: Critical evaluation of the use of laser diffraction for particle-size distribution analysis, *Soil Sci. Soc. Am. J.*, 68(3), 736–743, doi:10.2136/sssaj2004.7360, 2004.
- 500 Fox, L. E.: The solubility of colloidal ferric hydroxide and its relevance to iron concentrations in river water, *Geochim. Cosmochim. Acta*, 52(3), 771–777, doi:10.1016/0016-7037(88)90337-7, 1988.
- Froelich, P. N.: Kinetic control of dissolved phosphate in natural rivers and estuaries: A primer on the phosphate buffer mechanism, *Limnol. Oceanogr.*, 33(4.2), 649–668, 1988.
- Gérard, F.: Clay minerals, iron/aluminum oxides, and their contribution to phosphate sorption in soils — A myth revisited, 505 *Geoderma*, 262, 213–226, doi:10.1016/j.geoderma.2015.08.036, 2016.
- Goldberg, S. and Sposito, G.: A chemical model of phosphate adsorption by soils: I. Reference oxide minerals, *Soil Sci. Soc. Am. J.*, 48(4), 772–778, doi:10.2136/sssaj1984.03615995004800040015x, 1984.
- Golterman, H. L.: The calcium- and iron bound phosphate phase diagram, *Hydrobiol.*, 159(2), 149–151, doi:10.1007/BF00014722, 1988.
- 510 Golterman, H. L.: *The chemistry of phosphate and nitrogen compounds in sediments*, Kluwer Academic Publishers, Dordrecht, The Netherlands., 2004.
- Gottselig, N., Amelung, W., Kirchner, J. W., Bol, R., Eugster, W., Granger, S. J., Hernández-Crespo, C., Herrmann, F., Keizer, J. J., Korkiakoski, M., Laudon, H., Lehner, I., Löfgren, S., Lohila, A., Macleod, C. J. A., Mölder, M., Müller, C., Nasta, P., Nischwitz, V., Paul-Limoges, E., Pierret, M. C., Pilegaard, K., Romano, N., Sebastià, M. T., Stähli, M., Voltz, M., Vereecken, 515 H., Siemens, J. and Klumpp, E.: Elemental composition of natural nanoparticles and fine colloids in European forest stream waters and their role as phosphorus carriers, *Global Biogeochem. Cycles*, 31(10), 1592–1607, doi:10.1002/2017GB005657, 2017.
- Gran, G.: Determination of the equivalence point in potentiometric titrations. Part II, *Analyst*, 77(920), 661–671, doi:10.1039/AN9527700661, 1952.
- 520 Griffiths, N. A. and Johnson, L. T.: Influence of dual nitrogen and phosphorus additions on nutrient uptake and saturation kinetics in a forested headwater stream, *Freshw. Sci.*, 000–000, doi:10.1086/700700, 2018.
- van der Grift, B., Rozemeijer, J. C., Griffioen, J. and van der Velde, Y.: Iron oxidation kinetics and phosphate immobilization along the flow-path from groundwater into surface water, *Hydrol. Earth Syst. Sci.*, 18(11), 4687–4702, doi:https://doi.org/10.5194/hess-18-4687-2014, 2014.
- 525 Haggard, B. E. and Sharpley, A. N.: *Phosphorus transport in streams: Processes and modeling considerations*, in *Modeling phosphorus in the environment*, CRC Press, Boca Raton, FL., 2007.
- Haggard, B. E., Stanley, E. H. and Storm, D. E.: Nutrient retention in a point-source-enriched stream, *J. N. Am. Benthol. Soc.*, 24(1), 29–47, doi:10.1899/0887-3593(2005)024<0029:NRIAPS>2.0.CO;2, 2005.
- 530 Hall, R. O., Bernhardt, E. S. and Likens, G. E.: Relating nutrient uptake with transient storage in forested mountain streams, *Limnol. Oceanogr.*, 47(1), 255–265, doi:10.4319/lo.2002.47.1.0255, 2002.



- Hall, R. O., Baker, M. A., Rosi-Marshall, E. J., Tank, J. L. and Newbold, J. D.: Solute-specific scaling of inorganic nitrogen and phosphorus uptake in streams, *Biogeosciences*, 10(11), 7323–7331, doi:https://doi.org/10.5194/bg-10-7323-2013, 2013.
- Halliday, S. J., Wade, A. J., Skeffington, R. A., Neal, C., Reynolds, B., Rowland, P., Neal, M. and Norris, D.: An analysis of long-term trends, seasonality and short-term dynamics in water quality data from Plynlimon, Wales, *Sci. Total Environ.*, 434, 186–200, doi:10.1016/j.scitotenv.2011.10.052, 2012.
- 535
- Harvey, J. W.: Hydrologic exchange flows and their ecological consequences in river corridors, in *Stream Ecosystems in a Changing Environment*, pp. 1–84, Academic Press, London, UK., 2016.
- He, Z. and Honeycutt, C. W.: A modified molybdenum blue method for orthophosphate determination suitable for investigating enzymatic hydrolysis of organic phosphates, *Commun. Soil Sci. Plant Anal.*, 36(9–10), 1373–1383, doi:10.1081/CSS-200056954, 2005.
- 540
- Herndon, E. M., Kinsman-Costello, L., Duroe, K. A., Mills, J., Kane, E. S., Sebestyen, S. D., Thompson, A. A. and Wullschlegel, S. D.: Iron (oxyhydr)oxides serve as phosphate traps in tundra and boreal peat soils, *J. Geophys. Res. Biogeosci.*, 124, doi:10.1029/2018JG004776, 2019.
- Hill, W. R., Fanta, S. E. and Roberts, B. J.: Quantifying phosphorus and light effects in stream algae, *Limnol. Oceanogr.*, 54(1), 368–380, doi:10.4319/lo.2009.54.1.0368, 2009.
- 545
- Hoffman, A. R., Armstrong, D. E., Lathrop, R. C. and Penn, M. R.: Characteristics and influence of phosphorus accumulated in the bed sediments of a stream located in an agricultural watershed, *Aquat. Geochem.*, 15(3), 371–389, doi:10.1007/s10498-008-9043-2, 2009.
- Hollander, M., Wolfe, D. A. and Chicken, E.: The one-way layout, in *Nonparametric Statistical Methods*, pp. 39–114, John Wiley & Sons., 2013.
- 550
- House, W. A.: The physico-chemical conditions for the precipitation of phosphate with calcium, *Environ. Technol.*, 20(7), 727–733, doi:10.1080/09593332008616867, 1999.
- House, W. A.: Geochemical cycling of phosphorus in rivers, *Appl. Geochem.*, 18(5), 739–748, doi:10.1016/S0883-2927(02)00158-0, 2003.
- 555
- Huang, H., Wang, Z., Chen, D., Xia, F., Shang, X., Liu, Y., Dahlgren, R. A. and Mei, K.: Influence of land use on the persistence effect of riverine phosphorus, *Hydrol. Processes*, 32(1), 118–125, doi:10.1002/hyp.11408, 2018.
- Jan, J., Borovec, J., Kopáček, J. and Hejzlar, J.: What do results of common sequential fractionation and single-step extractions tell us about P binding with Fe and Al compounds in non-calcareous sediments?, *Water Res.*, 47(2), 547–557, doi:10.1016/j.watres.2012.10.053, 2013.
- 560
- Jan, J., Borovec, J., Kopáček, J. and Hejzlar, J.: Assessment of phosphorus associated with Fe and Al (hydr)oxides in sediments and soils, *J. Soils Sediments*, 15(7), 1620–1629, doi:10.1007/s11368-015-1119-1, 2015.
- Jarvie, H. P., Withers, P. J. A. and Neal, C.: Review of robust measurement of phosphorus in river water: sampling, storage, fractionation and sensitivity, *Hydrol. Earth Syst. Sci.*, 6(1), 113–131, doi:10.5194/hess-6-113-2002, 2002.
- 565
- Jarvie, H. P., Jürgens, M. D., Williams, R. J., Neal, C., Davies, J. J. L., Barrett, C., White, J., Jarvie, H. P., Ju, M. D., Davies, J. J. L., Barrett, C. and White, J.: Role of river bed sediments as sources and sinks of phosphorus across two major eutrophic



- UK river basins: the Hampshire Avon and Herefordshire Wye, *J. Hydrol.*, 304(1), 51–74, doi:10.1016/j.jhydrol.2004.10.002, 2005.
- 570 Jarvie, H. P., Neal, C., Jürgens, M. D., Sutton, E. J., Neal, M., Wickham, H. D., Hill, L. K., Harman, S. A., Davies, J. J. L., Warwick, A., Barrett, C., Griffiths, J., Binley, A., Swannack, N. and McIntyre, N.: Within-river nutrient processing in Chalk streams: The Pang and Lambourn, UK, *J. Hydrol.*, 330(1), 101–125, doi:10.1016/j.jhydrol.2006.04.014, 2006.
- Jarvie, H. P., Sharpley, A. N., Scott, J. T., Haggard, B. E., Bowes, M. J. and Massey, L. B.: Within-river phosphorus retention: accounting for a missing piece in the watershed phosphorus puzzle, *Environ. Sci. Technol.*, 46(24), 13284–13292, doi:10.1021/es303562y, 2012.
- 575 Jensen, H. S. and Thamdrup, B.: Iron-bound phosphorus in marine sediments as measured by bicarbonate-dithionite extraction, in *Proceedings of the Third International Workshop on Phosphorus in Sediments*, edited by P. C. M. Boers, Th. E. Cappenberg, and W. van Raaphorst, pp. 47–59, Springer Netherlands., 1993.
- Jensen, H. S., Kristensen, P., Jeppesen, E. and Skytthe, A.: Iron:phosphorus ratio in surface sediment as an indicator of phosphate release from aerobic sediments in shallow lakes, in *Sediment/Water Interactions*, edited by B. T. Hart and P. G. Sly, pp. 731–743, Springer Netherlands., 1992.
- 580 Kalbitz, K., Kaiser, K. and McDowell, W. H.: Nitrate decline unlikely to have triggered release of dissolved organic carbon and phosphate to streams, *Global Change Biol.*, 23(7), 2535–2536, doi:10.1111/gcb.13659, 2017.
- Konietschke, F., Hothorn, L. A. and Brunner, E.: Rank-based multiple test procedures and simultaneous confidence intervals, *Electron. J. Statist.*, 6, 738–759, doi:10.1214/12-EJS691, 2012.
- 585 Konietschke, F., Placzek, M., Schaarschmidt, F. and Hothorn, L. A.: nparcomp: An R software package for nonparametric multiple comparisons and simultaneous confidence intervals, *J. Stat. Software*, 64(1), 1–17, doi:10.18637/jss.v064.i09, 2015.
- Kronvang, B., Hoffmann, C. C. and Drøge, R.: Sediment deposition and net phosphorus retention in a hydraulically restored lowland river floodplain in Denmark: combining field and laboratory experiments, *Mar. Freshwater Res.*, 60(7), 638–646, doi:10.1071/MF08066, 2009.
- 590 Lair, G. J., Zehetner, F., Khan, Z. H. and Gerzabek, M. H.: Phosphorus sorption–desorption in alluvial soils of a young weathering sequence at the Danube River, *Geoderma*, 149(1–2), 39–44, doi:10.1016/j.geoderma.2008.11.011, 2009.
- Lewandowski, J. and Nützmann, G.: Nutrient retention and release in a floodplain’s aquifer and in the hyporheic zone of a lowland river, *Ecol. Eng.*, 36(9), 1156–1166, doi:10.1016/j.ecoleng.2010.01.005, 2010.
- Lijklema, L.: Interaction of orthophosphate with iron(III) and aluminum hydroxides, *Environ. Sci. Technol.*, 14(5), 537–541, doi:10.1021/es60165a013, 1980.
- 595 Lindsay, W. L.: *Chemical equilibria in soils.*, John Wiley and Sons Ltd., 1979.
- Lukkari, K., Hartikainen, H. and Leivuori, M.: Fractionation of sediment phosphorus revisited. I: Fractionation steps and their biogeochemical basis, *Limnol. Oceanogr. Methods*, 5(12), 433–444, doi:10.4319/lom.2007.5.433, 2007.
- 600 Machesky, M. L., Holm, T. R. and Slowikowski, J. A.: Phosphorus Speciation in Stream Bed Sediments from an Agricultural Watershed: Solid-Phase Associations and Sorption Behavior, *Aquat Geochem*, 16(4), 639–662, doi:10.1007/s10498-010-9103-2, 2010.



- Malá, J. and Lagová, M.: Comparison of digestion methods for determination of total phosphorus in river sediments, *Chem. Pap.*, 68(8), 1015–1021, doi:10.2478/s11696-014-0555-5, 2014.
- Marton, J. M. and Roberts, B. J.: Spatial variability of phosphorus sorption dynamics in Louisiana salt marshes, *J. Geophys. Res. Biogeosci.*, 119(3), 451–465, doi:10.1002/2013JG002486, 2014.
- 605 McCrackin, M. L., Muller-Karulis, B., Gustafsson, B. G., Howarth, R. W., Humborg, C., Svanbäck, A. and Swaney, D. P.: A century of legacy phosphorus dynamics in a large drainage basin, *Global Biogeochem. Cycles*, 32(7), 1107–1122, doi:10.1029/2018GB005914, 2018.
- McDaniel, M. D., David, M. B. and Royer, T. V.: Relationships between benthic sediments and water column phosphorus in Illinois streams., *J. Environ. Qual.*, 38(2), 607–617, doi:10.2134/jeq2008.0094, 2009.
- 610 McDowell, R. W.: Sediment phosphorus chemistry and microbial biomass along a lowland New Zealand stream, *Aquat. Geochem.*, 9(1), 19–40, doi:10.1023/B:AQUA.0000005620.15485.6d, 2003.
- McDowell, R. W.: Relationship between sediment chemistry, equilibrium phosphorus concentrations, and phosphorus concentrations at baseflow in rivers of the New Zealand National River Water Quality Network, *J. Environ. Qual.*, 44(3), 921–929, doi:10.2134/jeq2014.08.0362, 2015.
- 615 McDowell, R. W., Biggs, B. J. F., Sharpley, A. N. and Nguyen, L.: Connecting phosphorus loss from agricultural landscapes to surface water quality, *Chem. Ecol.*, 20(1), 1–40, doi:10.1080/02757540310001626092, 2004.
- McDowell, R. W., Snelder, T. H., Cox, N., Booker, D. J. and Wilcock, R. J.: Establishment of reference or baseline conditions of chemical indicators in New Zealand streams and rivers relative to present conditions, *Mar. Freshwater Res.*, 64(5), 387–400, doi:10.1071/MF12153, 2013.
- 620 McDowell, R. W., Cox, N., Daughney, C. J., Wheeler, D. and Moreau, M.: A national assessment of the potential linkage between soil, and surface and groundwater concentrations of phosphorus, *J. Am. Water Resour. Assoc.*, 51(4), 992–1002, doi:10.1111/1752-1688.12337, 2015.
- McDowell, R. W., Simpson, Z. P., Stenger, R. and Depree, C.: The influence of a flood event on the potential sediment control of baseflow phosphorus concentrations in an intensive agricultural catchment, *J Soils Sediments*, 19(1), 429–438, doi:10.1007/s11368-018-2063-7, 2019.
- 625 Meals, D. W., Dressing, S. A. and Davenport, T. E.: Lag time in water quality response to best management practices: a review, *J. Environ. Qual.*, 39(1), 85–96, doi:10.2134/jeq2009.0108, 2010.
- Mendes, L. R. D., Tonderski, K. and Kjaergaard, C.: Phosphorus accumulation and stability in sediments of surface-flow constructed wetlands, *Geoderma*, 331, 109–120, doi:10.1016/j.geoderma.2018.06.015, 2018.
- 630 Monbet, P., D. McKelvie, I. and J. Worsfold, P.: Sedimentary pools of phosphorus in the eutrophic Tamar estuary (SW England), *J. Environ. Monit.*, 12(1), 296–304, doi:10.1039/B911429G, 2010.
- Mulholland, P. J., Marzolf, E. R., Webster, J. R., Hart, D. R. and Hendricks, S. P.: Evidence that hyporheic zones increase heterotrophic metabolism and phosphorus uptake in forest streams, *Limnol. Oceanogr.*, 42(3), 443–451, doi:10.4319/lo.1997.42.3.0443, 1997.
- 635 Murphy, J. and Riley, J. P.: A modified single solution method for the determination of phosphate in natural waters, *Anal. Chim. Acta*, 27, 31–36, doi:10.1016/S0003-2670(00)88444-5, 1962.



- Muscarella, M. E., Bird, K. C., Larsen, M. L., Placella, S. A. and Lennon, J. T.: Phosphorus resource heterogeneity in microbial food webs, *Aquat. Microb. Ecol.*, 73(3), 259–272, 2014.
- 640 Nagul, E. A., McKelvie, I. D., Worsfold, P. and Kolev, S. D.: The molybdenum blue reaction for the determination of orthophosphate revisited: Opening the black box, *Anal. Chim. Acta*, 890, 60–82, doi:10.1016/j.aca.2015.07.030, 2015.
- Neal, C., Jarvie, H. P., Williams, R. J., Neal, M., Wickham, H. and Hill, L.: Phosphorus-calcium carbonate saturation relationships in a lowland chalk river impacted by sewage inputs and phosphorus remediation: an assessment of phosphorus self-cleansing mechanisms in natural waters, *Sci. Total Environ.*, 282–283, 295–310, doi:10.1016/S0048-9697(01)00920-2, 2002.
- 645 Newbold, J. D., Elwood, J. W., O'Neill, R. V. and Sheldon, A. L.: Phosphorus dynamics in a woodland stream ecosystem: a study of nutrient spiralling, *Ecology*, 64(5), 1249–1265, 1983.
- Nimick, D. A., Gammons, C. H. and Parker, S. R.: Diel biogeochemical processes and their effect on the aqueous chemistry of streams: A review, *Chem. Geol.*, 283(1), 3–17, doi:10.1016/j.chemgeo.2010.08.017, 2011.
- 650 Ohno, T. and Zibilske, L. M.: Determination of low concentrations of phosphorus in soil extracts using malachite green, *Soil Sci. Soc. Am. J.*, 55, 892–895, 1991.
- Packman, A. I. and Salehin, M.: Relative roles of stream flow and sedimentary conditions in controlling hyporheic exchange, *Hydrobiol.*, 494, 291–297, doi:10.1023/A:1025403424063, 2003.
- Parfitt, R. L.: Anion Adsorption by Soils and Soil Materials, in *Advances in Agronomy*, vol. 30, edited by N. C. Brady, pp. 1–50, Academic Press., 1979.
- 655 Parkhurst, D. L. and Appelo, C. A. J.: Description of input and examples for PHREEQC version 3: a computer program for speciation, batch-reaction, one-dimensional transport, and inverse geochemical calculations, USGS Numbered Series, U.S. Geological Survey, Reston, VA. [online] Available from: <http://pubs.er.usgs.gov/publication/tm6A43> (Accessed 9 November 2018), 2013.
- 660 Parsons, C. T., Rezanezhad, F., O'Connell, D. W. and Cappellen, P. V.: Sediment phosphorus speciation and mobility under dynamic redox conditions, *Biogeosciences*, 14(14), 3585–3602, doi:https://doi.org/10.5194/bg-14-3585-2017, 2017.
- Pierzynski, G. M., McDowell, R. W. and Sims, J. T.: Chemistry, Cycling, and Potential Movement of Inorganic Phosphorus in Soils, in *Phosphorus: Agriculture and the Environment*, pp. 53–86, American Society of Agronomy, Madison, WI., 2005.
- Plant, L. J. and House, W. A.: Precipitation of calcite in the presence of inorganic phosphate, *Colloids Surf., A*, 203(1), 143–153, doi:10.1016/S0927-7757(01)01089-5, 2002.
- 665 Postma, D.: The reactivity of iron oxides in sediments: A kinetic approach, *Geochim. Cosmochim. Acta*, 57(21), 5027–5034, doi:10.1016/S0016-7037(05)80015-8, 1993.
- Powers, S. M., Bruulsema, T. W., Burt, T. P., Chan, N. I., Elser, J. J., Haygarth, P. M., Howden, N. J. K., Jarvie, H. P., Lyu, Y., Peterson, H. M., Sharpley, A. N., Shen, J., Worrall, F. and Zhang, F.: Long-term accumulation and transport of anthropogenic phosphorus in three river basins, *Nat. Geosci.*, 9(5), 353–356, doi:10.1038/ngeo2693, 2016.
- 670 R Core Team: R: A language and environment for statistical computing, R Foundation for Statistical Computing, Vienna, Austria. [online] Available from: <https://www.r-project.org/>, 2018.



- Ren, J. and Packman, A. I.: Coupled stream-subsurface exchange of colloidal hematite and dissolved zinc, copper, and phosphate, *Environ. Sci. Technol.*, 39(17), 6387–6394, doi:10.1021/es050168q, 2005.
- 675 Rhoton, F. E., Bigham, J. M. and Lindbo, D. L.: Properties of iron oxides in streams draining the Loess Uplands of Mississippi, *Appl. Geochem.*, 17(4), 409–419, doi:10.1016/S0883-2927(01)00112-3, 2002.
- Rothe, M., Frederichs, T., Eder, M., Kleeberg, A. and Hupfer, M.: Evidence for vivianite formation and its contribution to long-term phosphorus retention in a recent lake sediment: a novel analytical approach, *Biogeosciences*, 11(18), 5169–5180, doi:https://doi.org/10.5194/bg-11-5169-2014, 2014.
- 680 Rounds, S. A.: Alkalinity and acid neutralizing capacity, in *National field manual for the collection of water-quality data*, vol. 9, edited by F. D. Wilde and D. B. Radtke, pp. 1–45, U.S. Geological Survey, Reston, Virginia. [online] Available from: <https://water.usgs.gov/owq/FieldManual/Chapter6/section6.6/>, 2012.
- Runkel, R. L., Kimball, B. A., McKnight, D. M. and Bencala, K. E.: Reactive solute transport in streams: A surface complexation approach for trace metal sorption, *Water Resour. Res.*, 35(12), 3829–3840, doi:10.1029/1999WR900259, 1999.
- 685 Sauer, D., Saccone, L., Conley, D. J., Herrmann, L. and Sommer, M.: Review of methodologies for extracting plant-available and amorphous Si from soils and aquatic sediments, *Biogeochemistry*, 80(1), 89–108, doi:10.1007/s10533-005-5879-3, 2006.
- Saunders, W. M. H.: Phosphate retention by New Zealand soils and its relationship to free sesquioxides, organic matter, and other soil properties, *N. Z. J. Agric. Res.*, 8(1), 30–57, doi:10.1080/00288233.1965.10420021, 1965.
- Senn, A.-C., Kaegi, R., Hug, S. J., Hering, J. G., Mangold, S. and Voegelin, A.: Composition and structure of Fe(III)-precipitates formed by Fe(II) oxidation in water at near-neutral pH: Interdependent effects of phosphate, silicate and Ca, *Geochim. Cosmochim. Acta*, 162, 220–246, doi:10.1016/j.gca.2015.04.032, 2015.
- 690 Sharpley, A., Jarvie, H. P., Buda, A., May, L., Spears, B. and Kleinman, P.: Phosphorus legacy: Overcoming the effects of past management practices to mitigate future water quality impairment, *J. Environ. Qual.*, 42(5), 1308–1326, doi:10.2134/jeq2013.03.0098, 2013.
- Shmueli, G.: To Explain or to Predict?, *Statist. Sci.*, 25(3), 289–310, doi:10.1214/10-STS330, 2010.
- 695 Simpson, Z. P., McDowell, R. W. and Condon, L. M.: The error in stream sediment phosphorus fractionation and sorption properties effected by drying pretreatments, *J Soils Sediments*, 19(3), 1587–1597, doi:10.1007/s11368-018-2180-3, 2019.
- Smolders, E., Baetens, E., Verbeeck, M., Nawara, S., Diels, J., Verdrievael, M., Peeters, B., De Cooman, W. and Baken, S.: Internal loading and redox cycling of sediment iron explain reactive phosphorus concentrations in lowland rivers, *Environ. Sci. Technol.*, 51(5), 2584–2592, doi:10.1021/acs.est.6b04337, 2017.
- 700 Snelder, T. H. and Biggs, B. J. F.: Multiscale river environment classification for water resources management, *J. Am. Water Resour. Assoc.*, 38(5), 1225–1239, doi:10.1111/j.1752-1688.2002.tb04344.x, 2002.
- Sø, H. U., Postma, D., Jakobsen, R. and Larsen, F.: Sorption of phosphate onto calcite; results from batch experiments and surface complexation modeling, *Geochim. Cosmochim. Acta*, 75(10), 2911–2923, doi:10.1016/j.gca.2011.02.031, 2011.
- 705 Stets, E. G., Butman, D., McDonald, C. P., Stackpoole, S. M., DeGrandpre, M. D. and Striegl, R. G.: Carbonate buffering and metabolic controls on carbon dioxide in rivers, *Global Biogeochem. Cycles*, 31(4), 663–677, doi:10.1002/2016GB005578, 2017.



- Stookey, L. L.: Ferrozine - a New Spectrophotometric Reagent for Iron, *Anal. Chem.*, 42(7), 779–, doi:10.1021/ac60289a016, 1970.
- 710 Stumm, W. and Morgan, J. J.: *Aquatic Chemistry: Chemical Equilibria and Rates in Natural Waters*, Third., John Wiley & Sons, New York., 1996.
- Stumm, W. and Sulzberger, B.: The cycling of iron in natural environments: Considerations based on laboratory studies of heterogeneous redox processes, *Geochim. Cosmochim. Acta*, 56(8), 3233–3257, doi:10.1016/0016-7037(92)90301-X, 1992.
- Stutter, M. I., Demars, B. O. L. L. and Langan, S. J.: River phosphorus cycling: Separating biotic and abiotic uptake during short-term changes in sewage effluent loading, *Water Res.*, 44(15), 4425–4436, doi:10.1016/j.watres.2010.06.014, 2010.
- 715 Venables, W. N. and Ripley, B. D.: *Modern applied statistics with S-PLUS*, Fourth., Springer, New York. [online] Available from: <http://www.stats.ox.ac.uk/pub/MASS4>, 2002.
- Viollier, E., Inglett, P. W., Hunter, K., Roychoudhury, a N. and Van Cappellen, P.: The ferrozine method revisited: Fe (II)/Fe (III) determination in natural waters, *Appl. Geochem.*, 15(6), 785–790, doi:10.1016/S0883-2927(99)00097-9, 2000.
- 720 Wauchope, R. D. and McDowell, L. L.: Adsorption of phosphate, arsenate, methanearsonate, and cacodylate by lake and stream sediments: Comparisons with soils, *J. Environ. Qual.*, 13(3), 499–504, doi:10.2134/jeq1984.00472425001300030034x, 1984.
- Weigelhofer, G., Ramião, J. P., Pitzl, B., Bondar-Kunze, E. and O’Keeffe, J.: Decoupled water-sediment interactions restrict the phosphorus buffer mechanism in agricultural streams, *Sci. Total Environ.*, 628–629, 44–52, doi:10.1016/j.scitotenv.2018.02.030, 2018.
- 725 Wohl, E.: Legacy effects on sediments in river corridors, *Earth Sci. Rev.*, 147, 30–53, doi:10.1016/j.earscirev.2015.05.001, 2015.
- Wood, S. A., Depree, C., Brown, L., McAllister, T. and Hawes, I.: Entrapped sediments as a source of phosphorus in epilithic cyanobacterial proliferations in low nutrient rivers, *PLOS ONE*, 10(10), e0141063, doi:10.1371/journal.pone.0141063, 2015.
- 730 Zak, D., Kleeberg, A. and Hupfer, M.: Sulphate-mediated phosphorus mobilization in riverine sediments at increasing sulphate concentration, *River Spree, NE Germany, Biogeochemistry*, 80(2), 109–119, doi:10.1007/s10533-006-0003-x, 2006.
- Zhang, J. Z. and Huang, X. L.: Relative importance of solid-phase phosphorus and iron on the sorption behavior of sediments, *Environ. Sci. Technol.*, 41(8), 2789–2795, doi:10.1021/es061836q, 2007.
- Zhang, J. Z., Fischer, C. J. and Ortner, P. B.: Optimization of performance and minimization of silicate interference in continuous flow phosphate analysis, *Talanta*, 49(2), 293–304, doi:10.1016/S0039-9140(98)00377-4, 1999.
- 735 Zhou, A., Tang, H. and Wang, D.: Phosphorus adsorption on natural sediments: Modeling and effects of pH and sediment composition, *Water Res.*, 39(7), 1245–1254, doi:10.1016/j.watres.2005.01.026, 2005.



740

**Table 1. Experimental procedure of the sequential sediment P fractionation, following the method of Jan et al. (2015); the targeted biogeochemical pools of P are given, but are not exact since fractionation methods are operationally defined. P and Fe analyses in the BD and NaOH fractions refer to total P and Fe. †Not applicable**

| Step or fraction         | Solution               | Extraction Time | Analyses        | Primary biogeochemical pool                                     |
|--------------------------|------------------------|-----------------|-----------------|---|
| <b>1. H<sub>2</sub>O</b> | D.I. water             | 30 min          | P               | Labile, loosely-bound P   |
| <b>2. BD-I</b>           | Bicarbonate-dithionite | 5 + 5 min       | P, Fe           | Less-crystalline, surface-active Fe oxides                      |
| <b>3. BD-II</b>          | Bicarbonate-dithionite | 2 h             | P, Fe           | Crystalline, poorly active Fe oxides                            |
| <b>Wash</b>              | NaCl                   | 5 min           | NA <sup>†</sup> | NA  |
| <b>4. NaOH-I</b>         | NaOH                   | 5 + 5 min       | P, Fe           | Active Al oxides, labile organic matter, clay minerals          |
| <b>5. NaOH-II</b>        | NaOH                   | 16 h            | P, Fe           | Crystalline Al oxides, refractory organic matter, clay minerals |
| <b>Wash</b>              | NaCl                   | 5 min           | NA              | NA  |
| <b>6. HCl</b>            | HCl                    | 24 h            | P               | Primary minerals  |



745

**Table 2. Summary of stream water chemistry grouped by River Environment Classification geology class; values are given as medians (means  $\pm$  standard deviation); lowercase letter exponents represent group-wise comparisons between geology classes (confidence level = 0.95).**

|                         | Units                                      | Geology Class                         |  |  |
|-------------------------|--|---------------------------------------|--|--|
|                         |  | Alluvium<br>( <i>n</i> =15)           | Sedimentary<br>( <i>n</i> =10)         | Volcanic basic<br>( <i>n</i> =6)       |
| <b>pH</b>               | S.U.                                       | 7.29 <sup>a</sup> (7.26 $\pm$ 0.33)   | 7.54 <sup>b</sup> (7.61 $\pm$ 0.22)    | 7.62 <sup>b</sup> (7.62 $\pm$ 0.06)    |
| <b>Conductivity</b>     | $\mu\text{S cm}^{-1}$                      | 142 (154 $\pm$ 51)                    | 78 (121 $\pm$ 79)                      | 155 (152 $\pm$ 18)                     |
| <b>Alkalinity</b>       | mg L <sup>-1</sup> as<br>CaCO <sub>3</sub> | 42.1 (44.3 $\pm$ 11.6)                | 31.4 (42.9 $\pm$ 23.8)                 | 39.4 (38.2 $\pm$ 6.8)                  |
| <b>DRP</b>              | $\mu\text{g L}^{-1}$                       | 7.4 <sup>b</sup> (10.8 $\pm$ 7.6)     | 5.0 <sup>a</sup> (5.6 $\pm$ 2.8)       | 27.7 <sup>c</sup> (26.9 $\pm$ 11.3)    |
| <b>NO<sub>3</sub>-N</b> | mg L <sup>-1</sup>                         | 1.947 <sup>b</sup> (1.857 $\pm$ 1.22) | 0.111 <sup>a</sup> (0.626 $\pm$ 1.18)  | 0.152 <sup>a</sup> (0.151 $\pm$ 0.080) |
| <b>SO<sub>4</sub></b>   | mg L <sup>-1</sup>                         | 8.21 <sup>b</sup> (8.44 $\pm$ 2.77)   | 4.89 <sup>b</sup> (9.38 $\pm$ 7.44)    | 3.54 <sup>a</sup> (3.49 $\pm$ 0.55)    |
| <b>Dissolved Fe</b>     | mg L <sup>-1</sup>                         | 0.011 <sup>a</sup> (0.06 $\pm$ 0.139) | 0.011 <sup>a</sup> (0.012 $\pm$ 0.006) | 0.137 <sup>b</sup> (0.153 $\pm$ 0.069) |
| <b>Dissolved Ca</b>     | mg L <sup>-1</sup>                         | 18.1 <sup>b</sup> (18.3 $\pm$ 5.52)   | 11.9 <sup>b</sup> (17.09 $\pm$ 9.8)    | 8.9 <sup>a</sup> (8.79 $\pm$ 1.33)     |



750

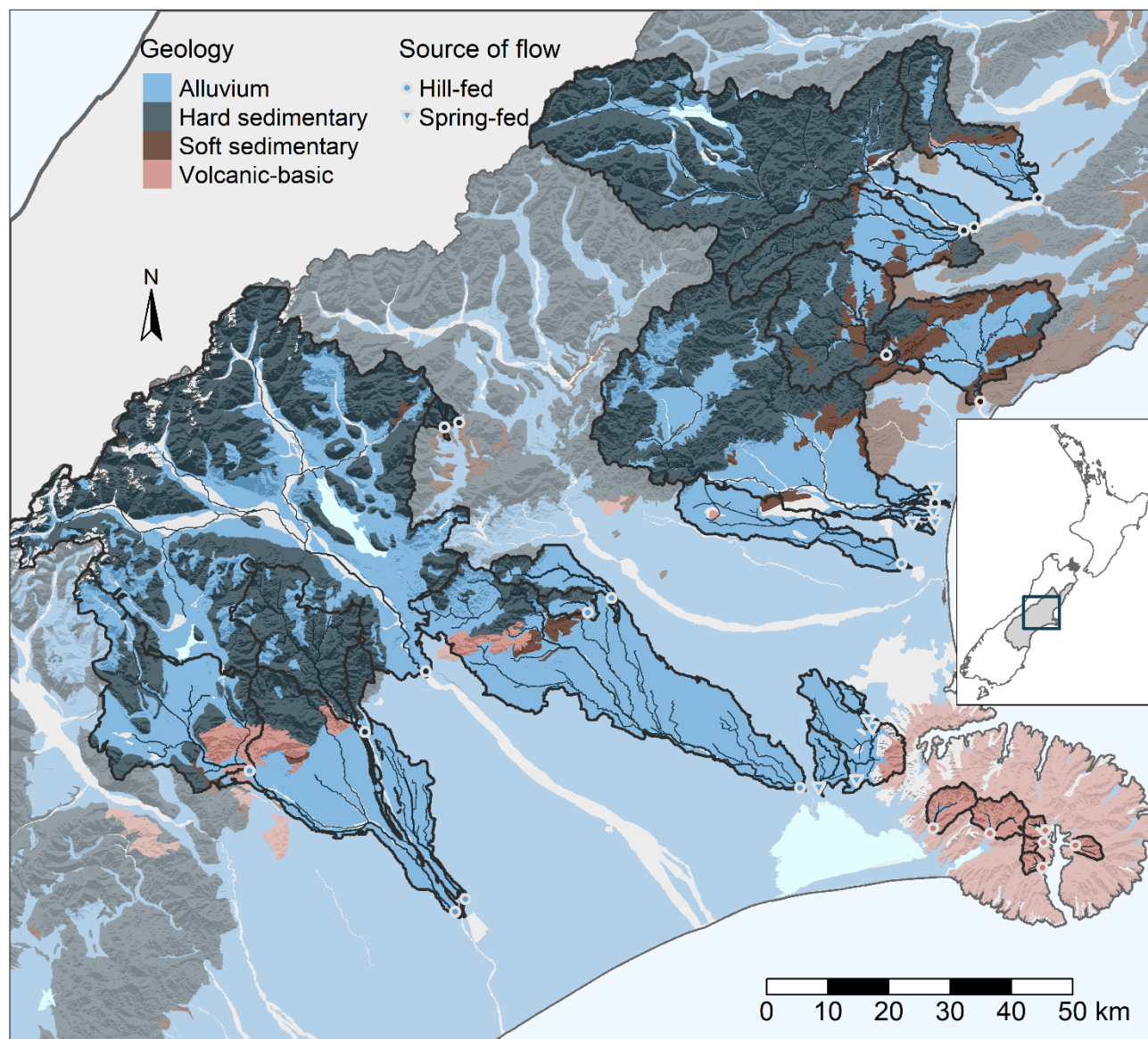
**Table 3.** Select physicochemical properties of the stream benthic sediments grouped by River Environment Classification geology class;  $D_{50}$  is the median particle size of the fine sediments (<2 mm); values are given as medians (means  $\pm$  standard deviation); lower case letter exponents represent group-wise comparisons between geology classes (confidence level = 0.95).

|                       | Units               | Geology Class                         |                                       |                                       |
|-----------------------|---------------------|---------------------------------------|---------------------------------------|---------------------------------------|
|                       |                     | Alluvium<br>( $n=15$ )                | Sedimentary<br>( $n=10$ )             | Volcanic basic<br>( $n=6$ )           |
| <b>pH</b>             | S.U.                | 6.93 <sup>a</sup> (6.91 $\pm$ 0.24)   | 7.12 <sup>ab</sup> (7.26 $\pm$ 0.46)  | 7.26 <sup>b</sup> (7.31 $\pm$ 0.26)   |
| <b>Total C</b>        | g kg <sup>-1</sup>  | 3.68 <sup>b</sup> (13.2 $\pm$ 17.9)   | 1.06 <sup>a</sup> (1.3 $\pm$ 0.58)    | 8.53 <sup>b</sup> (10.8 $\pm$ 5.9)    |
| <b>Total N</b>        | g kg <sup>-1</sup>  | 0.41 <sup>b</sup> (1.31 $\pm$ 1.69)   | 0.20 <sup>a</sup> (0.23 $\pm$ 0.12)   | 0.65 <sup>b</sup> (0.83 $\pm$ 0.43)   |
| <b>Total Al</b>       | g kg <sup>-1</sup>  | 20.15 <sup>a</sup> (21.93 $\pm$ 6.04) | 18.44 <sup>a</sup> (20.42 $\pm$ 4.88) | 35.39 <sup>b</sup> (37.2 $\pm$ 8.35)  |
| <b>Total Ca</b>       | g kg <sup>-1</sup>  | 5.77 <sup>a</sup> (6.25 $\pm$ 2.34)   | 5.97 <sup>ab</sup> (6.35 $\pm$ 2.21)  | 9.59 <sup>b</sup> (9.46 $\pm$ 2.14)   |
| <b>Total Fe</b>       | g kg <sup>-1</sup>  | 22.14 <sup>a</sup> (21.95 $\pm$ 4.05) | 23.31 <sup>a</sup> (23.44 $\pm$ 3.36) | 48.45 <sup>b</sup> (50.43 $\pm$ 5.93) |
| <b>Total Mn</b>       | mg kg <sup>-1</sup> | 379 <sup>a</sup> (455 $\pm$ 275)      | 372 <sup>a</sup> (368 $\pm$ 89.2)     | 725 <sup>b</sup> (713 $\pm$ 160)      |
| <b>Total P</b>        | mg kg <sup>-1</sup> | 548 <sup>a</sup> (597 $\pm$ 219)      | 476 <sup>a</sup> (462 $\pm$ 121)      | 2130 <sup>b</sup> (2220 $\pm$ 525)    |
| <b>Clay</b>           | % volume            | 0.011 <sup>b</sup> (0.99 $\pm$ 1.6)   | 0 <sup>a</sup> (0.001 $\pm$ 0.004)    | 0.3 <sup>b</sup> (0.5 $\pm$ 0.7)      |
| <b>Silt</b>           | % volume            | 5.25 <sup>b</sup> (19.8 $\pm$ 25.9)   | 0.049 <sup>a</sup> (0.98 $\pm$ 1.54)  | 14.7 <sup>b</sup> (16.8 $\pm$ 9.96)   |
| <b>Sand</b>           | % volume            | 94.7 <sup>a</sup> (79.2 $\pm$ 27.4)   | 99.9 <sup>b</sup> (99.0 $\pm$ 1.55)   | 85.0 <sup>a</sup> (82.7 $\pm$ 10.7)   |
| <b>D<sub>50</sub></b> | $\mu$ m             | 415 <sup>a</sup> (356 $\pm$ 255)      | 701 <sup>b</sup> (680 $\pm$ 232)      | 544 <sup>ab</sup> (491 $\pm$ 238)     |

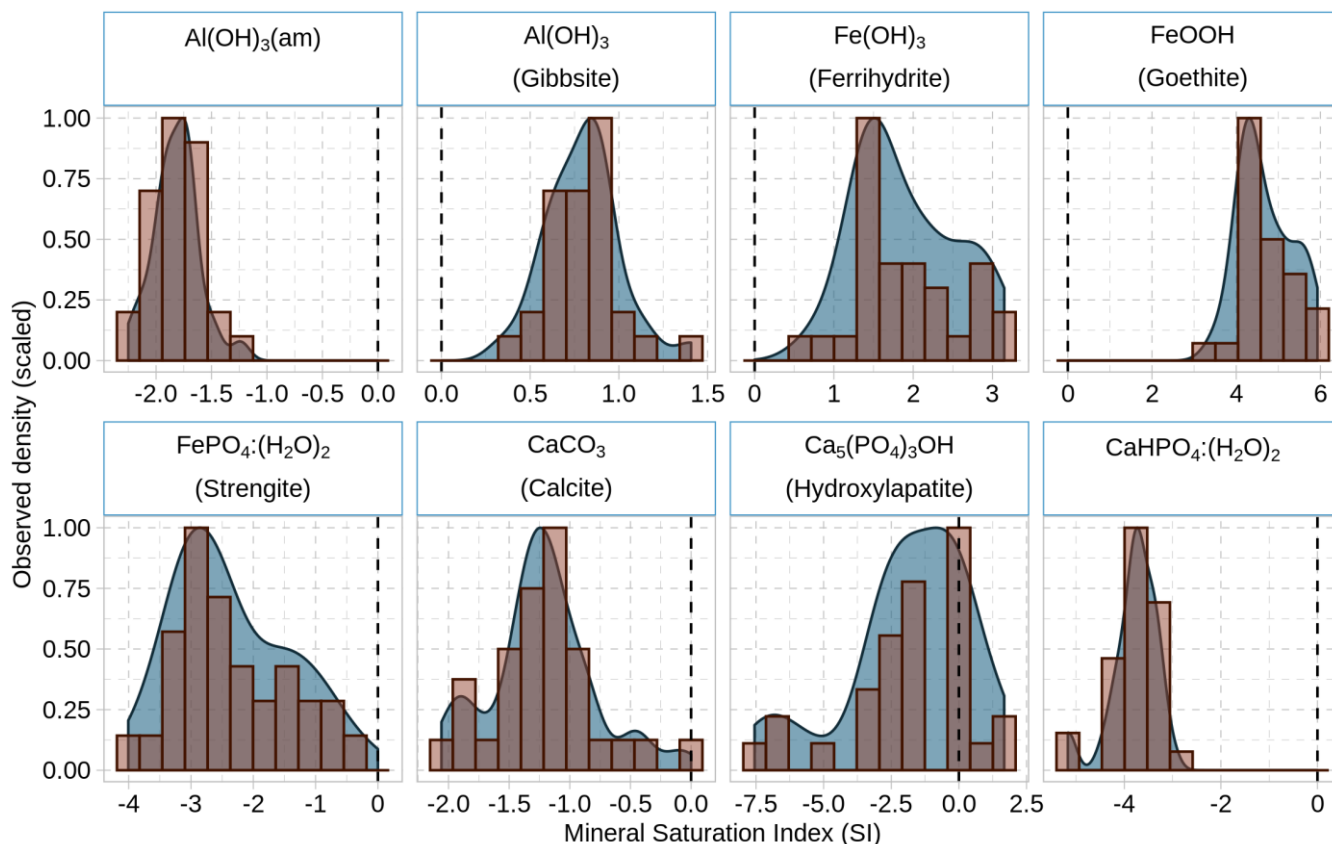


755 **Table 4. Stream sediment P fractions, Fe fractions, molar Fe:P ratios (including total Fe to total P), and sorption metrics. Values are given as medians (means ± standard deviation). The lowercase letter exponents represent group-wise comparisons between geology classes (confidence level = 0.95); for explanation of the sorption metrics, see Sect. 2.**

|                              |   | <b>Geology Class</b>             |                                    |                                 |
|------------------------------|---|----------------------------------|------------------------------------|---------------------------------|
| Units                        |   | Alluvium<br>(n=15)               | Sedimentary<br>(n=10)              | Volcanic basic<br>(n=6)         |
| <b>Sediment P fractions</b>  |   |                                  |                                    |                                 |
| <b>H<sub>2</sub>O</b>        | mg P kg <sup>-1</sup>   | 1.39 <sup>b</sup> (1.82 ± 1.41)  | 0.417 <sup>a</sup> (0.436 ± 0.081) | 2.48 <sup>b</sup> (3.84 ± 3.76) |
| <b>BD-I</b>                  |   | 27.8 <sup>b</sup> (52.1 ± 51.9)  | 4.14 <sup>a</sup> (3.62 ± 1.87)    | 31.8 <sup>b</sup> (40.4 ± 25.5) |
| <b>BD-II</b>                 |   | 14.8 <sup>b</sup> (32.2 ± 32.6)  | 3.53 <sup>a</sup> (2.98 ± 1.405)   | 38.4 <sup>b</sup> (37.2 ± 4.52) |
| <b>NaOH-I</b>                |   | 39.4 <sup>b</sup> (61.2 ± 60.3)  | 25.2 <sup>a</sup> (23.8 ± 7.11)    | 292 <sup>c</sup> (342 ± 185)    |
| <b>NaOH-II</b>               |   | 20.2 <sup>ab</sup> (30.6 ± 29.1) | 10.5 <sup>a</sup> (10.4 ± 4.79)    | 97.2 <sup>b</sup> (176 ± 177)   |
| <b>HCl</b>                   |   | 271 <sup>a</sup> (337 ± 163)     | 414 <sup>ab</sup> (452 ± 161)      | 1400 <sup>b</sup> (1370 ± 572)  |
| <b>Sediment Fe fractions</b> |   |                                  |                                    |                                 |
| <b>BD-I</b>                  | mg Fe kg <sup>-1</sup>  | 529 <sup>b</sup> (1360 ± 1500)   | 252 <sup>a</sup> (254 ± 66.1)      | 2480 <sup>c</sup> (2560 ± 623)  |
| <b>BD-II</b>                 |   | 664 <sup>a</sup> (915 ± 930)     | 433 <sup>a</sup> (446 ± 190)       | 5990 <sup>b</sup> (5150 ± 1670) |
| <b>NaOH-I</b>                |   | 50.4 <sup>b</sup> (92.98 ± 102)  | 21.7 <sup>a</sup> (22.6 ± 8.18)    | 107 <sup>c</sup> (118 ± 41.6)   |
| <b>NaOH-II</b>               |   | 447 <sup>b</sup> (122 ± 182)     | 35.9 <sup>a</sup> (36.2 ± 11.1)    | 99.6 <sup>b</sup> (131 ± 94.6)  |
| <b>Fe:P (molar)</b>          |   |                                  |                                    |                                 |
| <b>BD-I</b>                  | mol Fe mol P <sup>-1</sup>                                    | 15.5 <sup>a</sup> (18.3 ± 9.85)  | 36.4 <sup>b</sup> (65.01 ± 66.9)   | 39.1 <sup>b</sup> (40.6 ± 14.3) |
| <b>BD-II</b>                 |   | 19.9 <sup>a</sup> (31.6 ± 25.05) | 80.7 <sup>b</sup> (99.2 ± 61.01)   | 85.8 <sup>b</sup> (76.6 ± 21.6) |
| <b>NaOH-I</b>                |   | 0.71 <sup>a</sup> (1.15 ± 1.15)  | 0.52 <sup>b</sup> (0.59 ± 0.34)    | 0.23 <sup>b</sup> (0.25 ± 0.15) |
| <b>NaOH-II</b>               |   | 2.11 (2.69 ± 2.40)               | 1.80 (2.47 ± 1.63)                 | 0.38 (3.12 ± 6.25)              |
| <b>Total</b>                 |   | 22.3 <sup>b</sup> (22.2 ± 5.73)  | 28.4 <sup>c</sup> (29.1 ± 4.25)    | 13.3 <sup>a</sup> (13.1 ± 2.64) |
| <b>Sorption metrics</b>      |   |                                  |                                    |                                 |
| <b>ASC</b>                   | % P retention   | 14.3 <sup>b</sup> (33.6 ± 26.9)  | 6.98 <sup>a</sup> (10.2 ± 5.58)    | 49.4 <sup>b</sup> (49.4 ± 11.1) |
| <b>BWI</b>                   | $\frac{\text{mg P kg}^{-1}}{\log_{10}(\mu\text{g P L}^{-1})}$ | 12.7 <sup>b</sup> (51.95 ± 54.7) | 6.84 <sup>a</sup> (8.8 ± 5.57)     | 53.5 <sup>b</sup> (53.4 ± 12.3) |



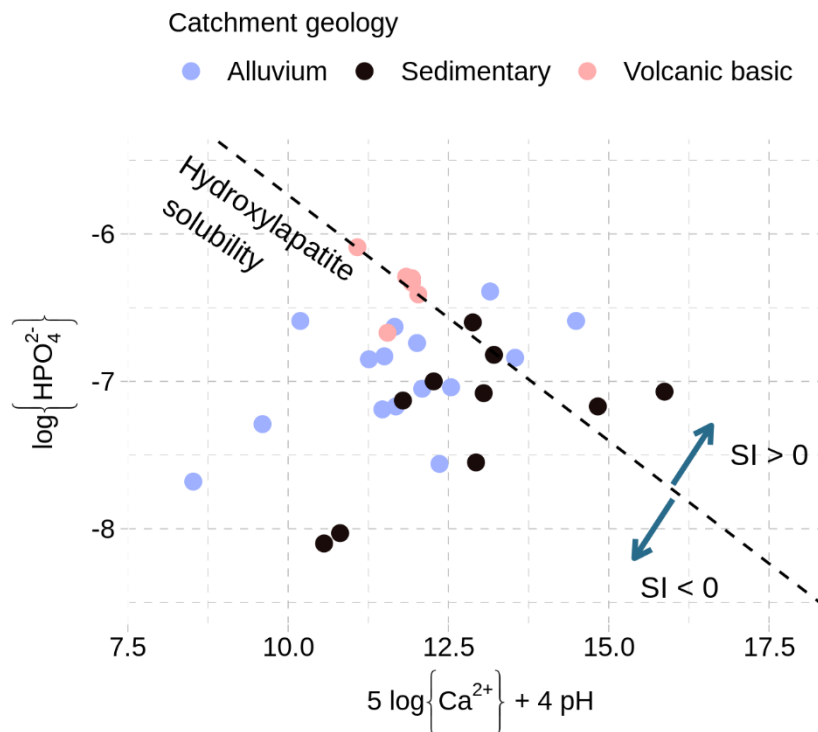
760 **Figure 1.** Study streams, and their catchments, in Canterbury, New Zealand (see inset). The geology classification used by the (New Zealand) River Environment Classification scheme is shown, with ‘Miscellaneous’ (loess, peat), ‘Other’ (river beds, ice cover, lakes, and urban centers), and Plutonic geology classes excluded for clarity. Sampling locations are shown, with circles indicating ‘Hill-fed’ streams (i.e., no major groundwater inputs) and triangles indicating ‘spring-fed’ streams.



765

**Figure 2. Distributions of select mineral saturation indices for the stream samples ( $n=31$ ), where positive (negative) saturation index (SI) indicates the thermodynamic potential for the mineral to precipitate (dissolve). The frequency distributions are displayed as normalized densities.  $SI=0$  is indicated on each sub-plot with a dashed vertical line. The solid phase chemical formulae are provided as given in the MINTEQ.v4 database.**

770



775 **Figure 3.** Log-activity of  $HPO_4^{2-}$  plotted against a function of log-activities of  $Ca^{2+}$  and  $H^+$  for the stream samples ( $n=31$ ). The dashed line is a reference solubility line for hydroxylapatite, where points below (above) this line are likely sub-saturated (super-saturated) with respect to hydroxylapatite.

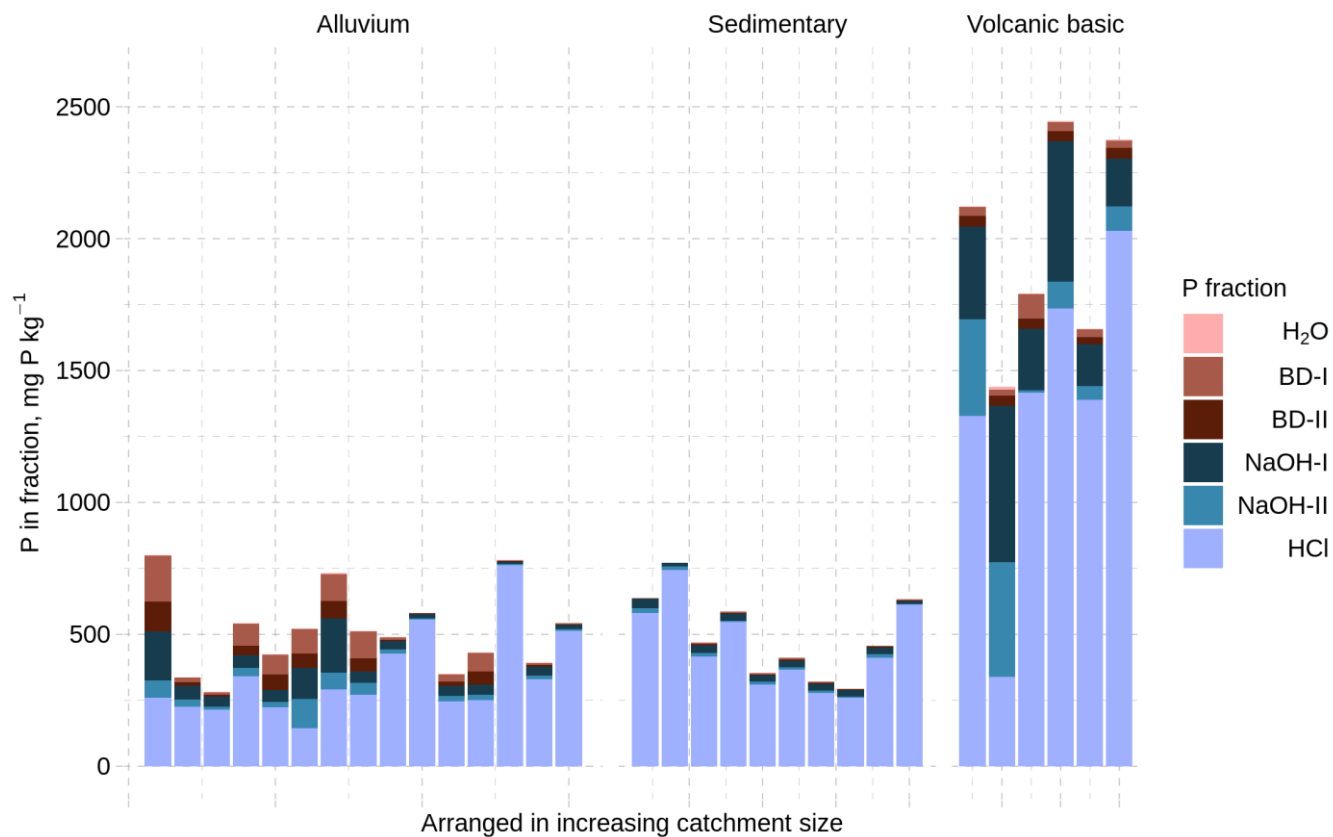
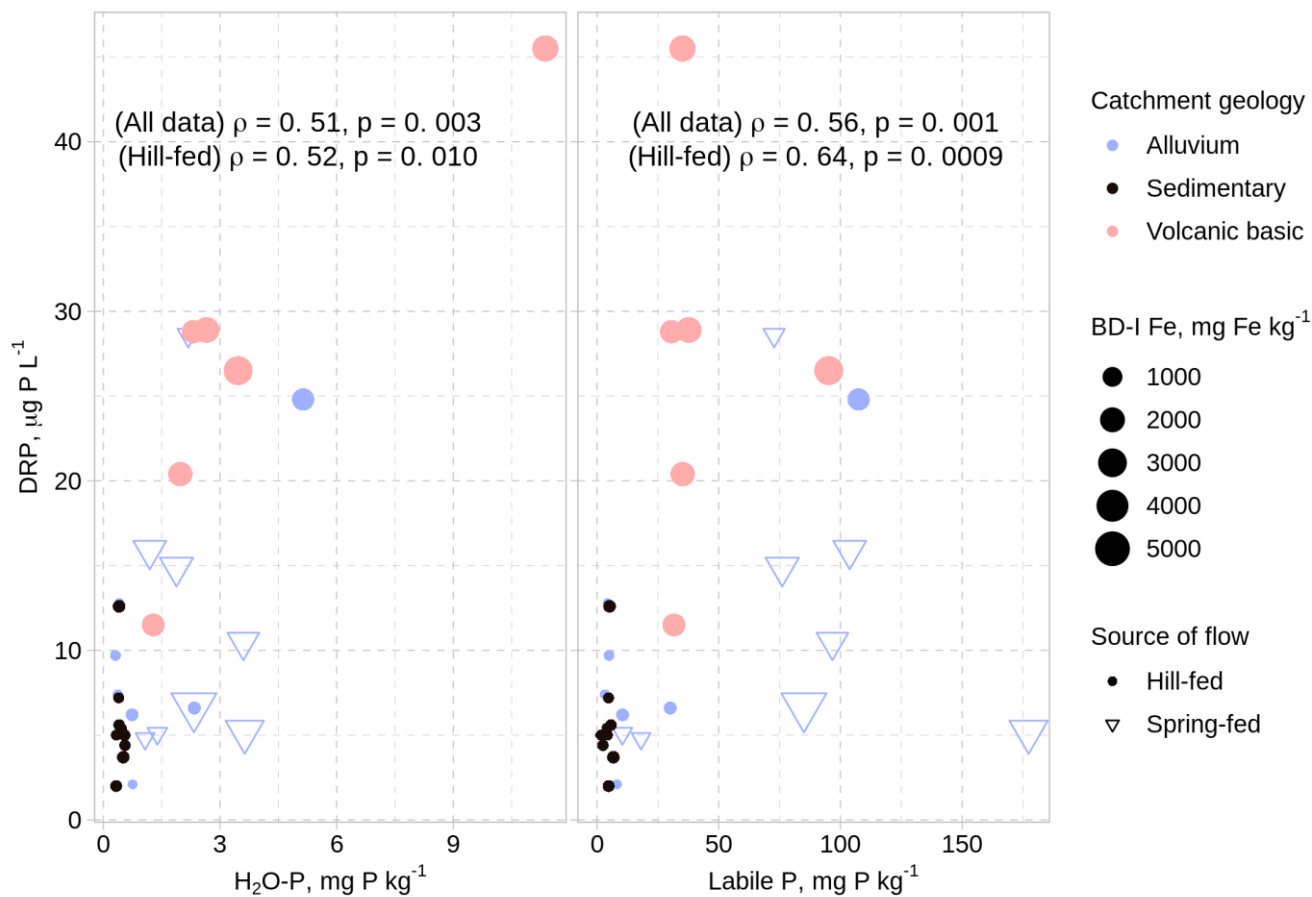
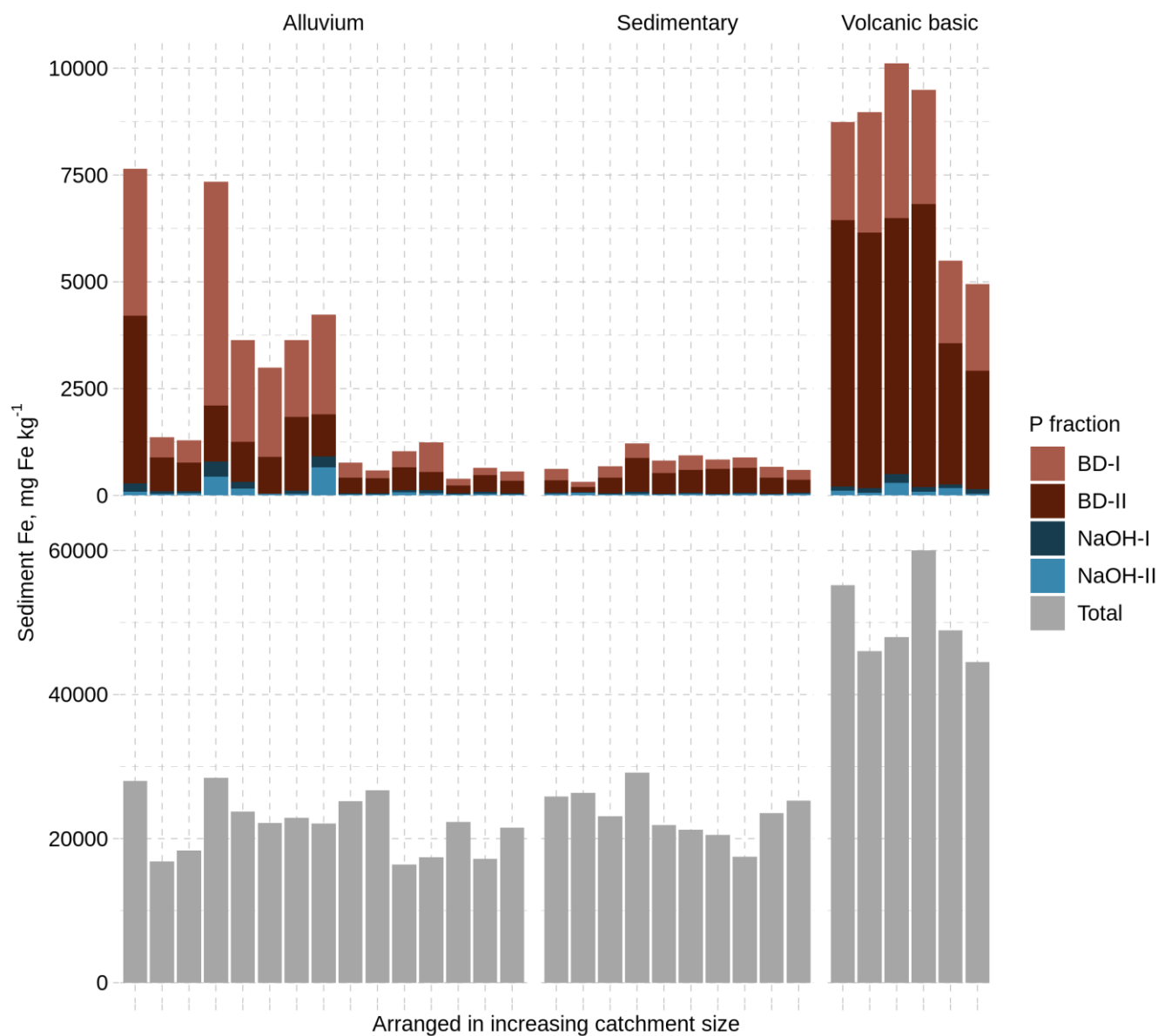


Figure 4. Benthic sediment (<2 mm) phosphorus content fractionated according to decreasing chemical lability; bars are arranged in increasing order of catchment size within the River Environment Classification geology class.



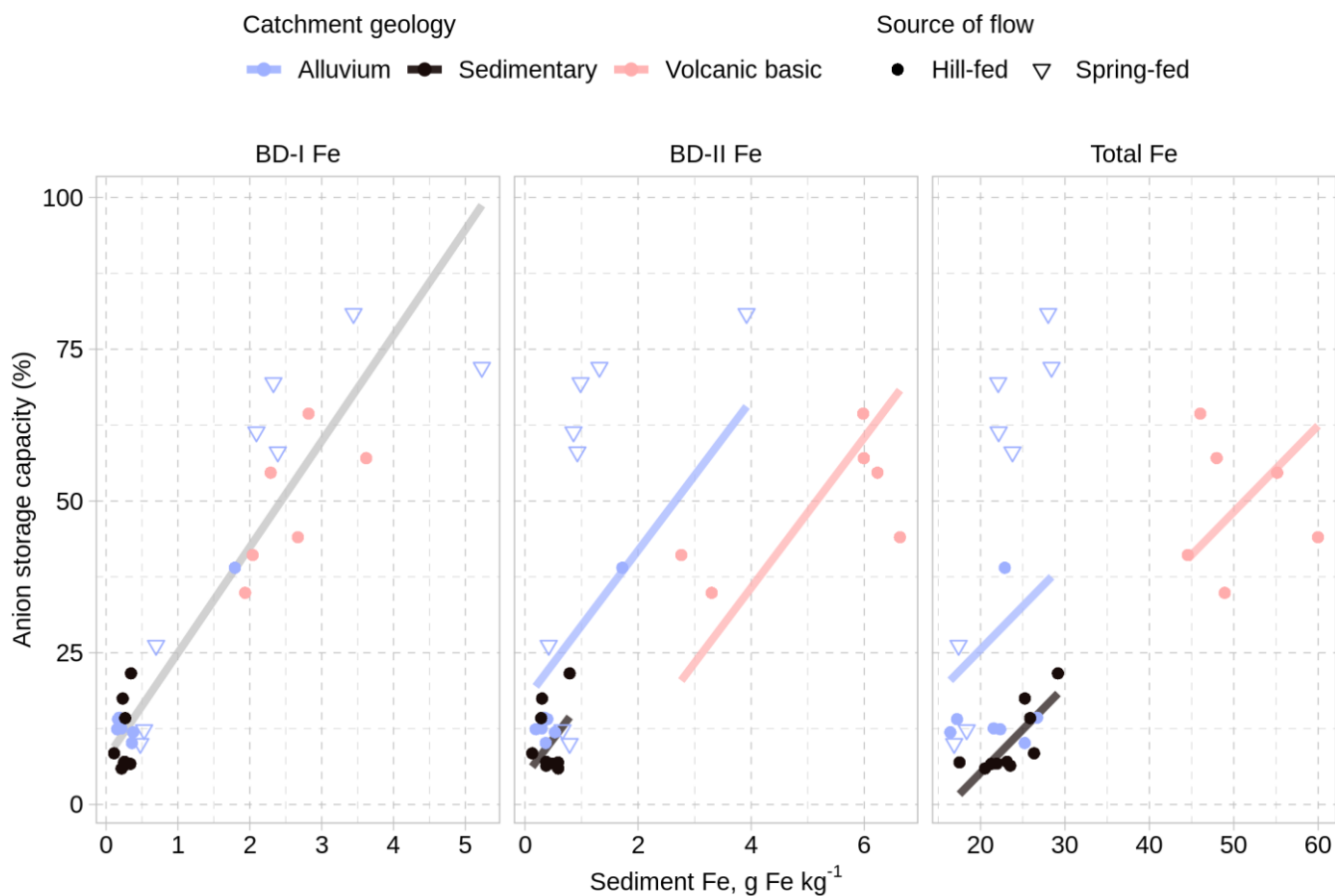
780

**Figure 5.** Stream DRP concentration as a function of sediment H<sub>2</sub>O-P and sediment labile P (H<sub>2</sub>O-P plus BD-I P) concentrations from the sequential P fractionations. Spearman correlation tests are shown for all data ( $n=31$ ) as well as for only hill-fed streams ( $n=23$ ).



785

**Figure 6. Sediment Fe concentration as measured in the P fractions (potentially reactive Fe arranged in decreasing lability; top row) or as the total Fe concentration (bottom row); note the differences in scale. Each bar (site) is arranged in increasing catchment size within the River Environment Classification geology class.**



790

**Figure 7.** Sediment P sorption potential as measured by anion storage capacity (ASC; %) as a function of sediment Fe in the bicarbonate-dithionite (BD) extractable pools and total sediment Fe. The optimal robust linear models for ASC with each Fe fraction, as discussed in text, are shown; note that while BD-I Fe alone predicts ASC, the models for BD-II Fe and total Fe include catchment geology as a covariate.

795

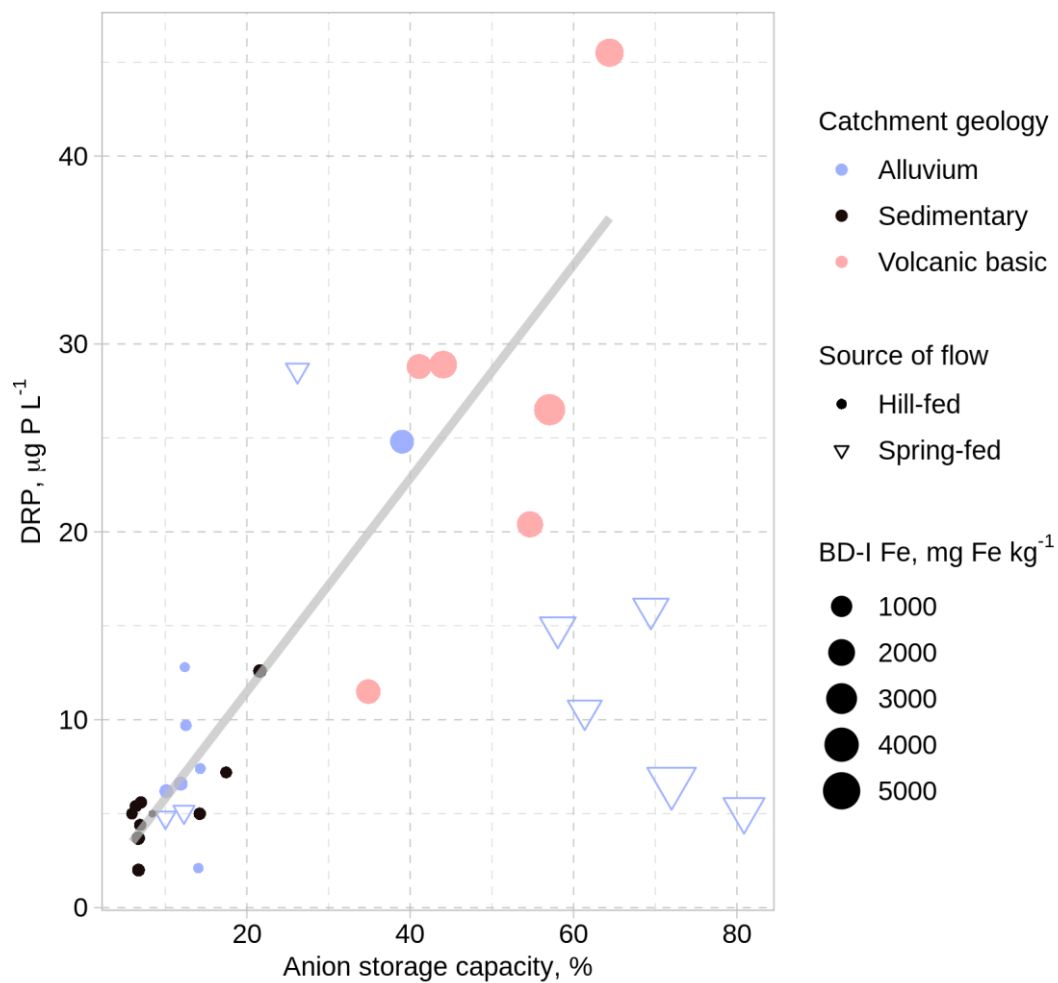


**Figure 8.** In-stream DRP as a function of sediment P sorption metrics (anion storage capacity (ASC; %) and Bache-Williams Index (BWI; refer to methods for unit interpretation)). The robust linear model discussed in text is shown.